Presentations by specialists on technical issues identified from previous studies of historical seismicity and fault sources at Yucca Mountain were the focus of the first day and a half of the workshop. These were followed by a day and a half of presentations on available and forthcoming data sets for the Yucca Mountain region. Topics included historical seismicity, regional and local faults, geologic mapping (both surficial and bedrock), geochronological, structural, and stratigraphic studies, and a variety of geophysical studies. Presentations were given by Yucca Mountain principal investigators who not only provided reference information for published data, but also offered to provide much of the unpublished data to the experts either through personal communications or the USGS Yucca Mountain Project Branch. Before the workshop, the USGS distributed a large amount of available data and lists of relevant data sources to each expert. A complete list of this material is included as Table 3 of the workshop summary (Appendix C).

3.2.2 Workshop #2-Seismic Hazard Methodologies

The workshop on Seismic Hazard Methodologies, October 16-18, 1996, was conducted after the project resumed following a 1-year hiatus. The purpose of this 2½-day workshop was twofold: (1) to review data that had become available since the project had stopped and (2) to identify and evaluate methods and approaches for characterizing seismic sources in the Yucca Mountain region. The workshop also served as a kickoff meeting for restarting the project, and participants were advised of revisions to the Project Plan and schedule.

The approach during the workshop was to divide seismic source characterization into two parts for vibratory ground motion analysis and fault displacement analysis. These parts were then further subdivided into three components: seismic source location and geometry, maximum earthquake magnitude, and earthquake recurrence assessment. Presentations by a variety of technical specialists, many of them experts, were given on each of these topics, first focusing on available methods for characterization and then describing newly available data. A complete list of the data provided is included as Table 1 in the workshop summary (Appendix C).

3.2.3 Workshop #3-Alternative Models and Interpretations and Field Trip

The workshop on Alternative Models and Interpretations, November 18-21, 1996, was combined with a field trip to Yucca Mountain, Crater Flat, and Bare Mountain. The purpose of the 4-day field trip and workshop was to review and evaluate alternative models, hypotheses, and interpretations that are important to the characterization of seismic sources in the Yucca Mountain region. The agenda for the workshop and field trip was developed with the explicit purpose of juxtaposing alternative ideas and views presented by various proponents. Discussions were facilitated to encourage the experts to probe for a better understanding of the technical bases for each model, to debate and listen to the pros and cons of the alternatives, and to quiz the proponents to better understand the uncertainties associated with each model. Additionally, the field trip enabled the experts to observe both surface and subsurface exposures at many key sites, providing first-hand insights into field data and interpretations. In this way they were able to evaluate the limits on resolution and the uncertainties associated with the field data and interpretations.

Throughout the workshop and field trip, a forum was provided for structured debate. Various scientists, including some experts, assumed the role of proponent in presenting arguments in favor of a particular model or interpretation. The experts were then encouraged to act as evaluators by probing the proponent positions in an effort to better understand the interpretations, the supporting data for each interpretation, and the associated uncertainties.

The field trip included 2½ days of field review and discussion focused on (1) the behavior of faults in the Yucca Mountain vicinity, (2) the nature of faulting in the potential repository block, and (3) the behavior of the Bare Mountain fault. John Whitney coordinated the field trip; individual stops were led by a variety of Yucca Mountain investigators. Numerous excavations and natural exposures were reviewed along many faults, including the Bare Mountain, Crater Flat, Windy Wash, Solitario Canyon, Ghost Dance, Bow Ridge, and Paintbrush Canyon faults. At these stops the principal investigators explained the field relationships, provided interpretations of the displacements, their ages, and recurrence, and expressed their uncertainties. A half-day trip into the ESF provided a subsurface view of faults and fractures in the proposed repository block. Highlights of this trip included exposures of (1) the Bow Ridge fault, (2) small intrablock reverse and normal faults, (3) cooling joints and faults, (4) the Drill Hole Wash fault, and (5) breccia zones.

The workshop discussions entailed presentations and debate centered around five key issues to seismic source and fault displacement characterization: tectonic models, three-dimensional geometry of faults, definition and synchronicity of faulting events, characterization of faulting in the proposed repository block, and maximum background earthquakes. Presentations of proponent positions on the five key issues were followed by debate by the experts. Some of the most extensive discussions focused on (1) the possible existence and character of large, buried strike-slip shear zones and detachment faults, (2) structural models of the subsurface geometry of the Bare Mountain and Yucca Mountain faults, (3) the occurrence of distributive faulting on multiple faults, possibly associated with volcanism, (4) slip rates on the Bare Mountain fault and implications to Yucca Mountain faults, (5) the origin of fracturing events observed in many exposures throughout Yucca Mountain, and (6) the age of youngest activity and Quaternary rates of activity for faults in Tertiary bedrock. A more comprehensive summary of the field trip itinerary and the issues discussed throughout the 4-day session is included in the workshop summary (Appendix C).

3.2.4 Workshop #4-Preliminary Interpretations

The goals of the Preliminary Interpretations Workshop, January 6-8, 1997, were to (1) provide an opportunity for the expert teams to receive feedback from their colleagues by presenting and discussing their preliminary interpretations regarding key issues, (2) train the expert teams in the process of elicitation and the characterization of uncertainty, and (3) present and discuss additional information and interpretations of importance to the study. To accomplish these goals, a series of presentations by the experts and group discussions were conducted. Five key issues were identified: (1) tectonic models, (2) potential seismic sources, (3) maximum magnitudes, (4) earthquake recurrence, and (5) fault displacement methodology. Two expert teams were assigned to present their preliminary interpretations of each issue. These presentations were followed by group discussion of each issue, during which the other teams were given the opportunity to debate the credibility of alternative views and to present their preliminary interpretations.

The focus of the presentations and discussions was on understanding the interpretations, their technical bases, their consistency or inconsistency with data, and the expression of uncertainty. Discussion was facilitated so that each team understood the interpretations of others, including the degree to which an interpretation was supported by earthquake and

faulting models and observed data. The experts could then more knowledgeably reevaluate their own team interpretations. The objective was to help teams prepare for the upcoming elicitation interviews so that interpretations would be well-reasoned, technically supported, and complete. Throughout this 2½-day workshop, the facilitator encouraged the experts to explore the issues thoroughly, ask questions that would help them during the elicitations, and continually keep in mind the characterization of uncertainties.

Also included in the workshop was a half-day elicitation training session conducted by normative expert Peter Morris, along with presentations by technical specialists of additional information on some key issues that were highlighted or outstanding from previous workshops. These included presentations on investigations of the Sundance fault, interpretations of seismic reflection lines and relevant geophysical data in the Yucca Mountain vicinity, the southern extent of Yucca Mountain faults, and the seismogenic potential of known or postulated shallow-dipping normal faults. More details on these presentations and those given by the teams on their preliminary interpretations are included in the workshop summary (Appendix C).

3.2.5 Workshop #5-Feedback

The Feedback Workshop, April 14-16, 1997, occurred after the elicitation interviews (discussed below). The purpose of the workshop was to provide feedback to the expert teams by (1) providing an opportunity for the teams to discuss the first round of their interpretations, (2) allowing each team to understand and ask questions about the interpretations made by other teams, (3) providing information on the derivative products of their first-round assessments (i.e., seismic source characteristics), and (4) providing sensitivity analyses to show the relative impact of various assessments on the calculated results. To accomplish these goals, a series of presentations and group discussions were conducted, with emphasis on facilitated interaction among the experts and feedback from the SFFD Facilitation and PSHA Calculations teams. For each of six key issues, two or three expert teams presented their interpretations, followed by a general discussion that included all of the teams. These six key issues, identified by the SSFD Facilitation Team from the preliminary results, included (1) characterization of areal seismic source zones, (2) geometry of local faults, (3) synchronous ruptures of local faults, (4) maximum magnitudes and recurrence on local faults, (5) characterization of other seismic sources, such as buried strike-

slip shear zones, detachments, volcanic zones, and other buried or postulated structures, and (6) methodologies for evaluating fault displacement.

The focus of the presentations and discussion was on understanding the interpretations of others, their technical bases, consistency with data, and expression of uncertainty. Preliminary results and sensitivity analyses were presented, highlighting the sources and parameters most significant to the analyses.

The specific aspects of the six issues discussed were (1) different approaches for defining and determining M_{max} for areal source zones containing Yucca Mountain (i.e., host zones), (2) processing and analysis of the historical seismicity catalog to estimate earthquake recurrence for host zones, (3) different approaches to determining seismogenic depths, (4) the use of structural and tectonic models to constrain subsurface geometries of local faults and potential buried seismic sources, (5) different approaches to developing models of rupture behavior for local faults, (6) the bases for assessing the potential activity of faults, and (7) different approaches to assessing the amounts and rates of fault slip for smaller (not block-bounding) faults in Tertiary bedrock within the Controlled Area. In regard to the latter, the experts extensively discussed the distinction between seismogenic or principal slip, distributive or secondary slip, and nontectonic slip. A clear and common understanding of this distinction is important, because some faults were included as potential sources of fault displacement, but were determined not to be independent seismogenic sources capable of generating earthquakes in the ground motion assessment.

During the workshop, feedback was also provided from the PSHA Calculations Team regarding preliminary results and sensitivity analyses for the first round of seismic source characterization and ground motion interpretations. Feedback included specific results for five teams' characterization models for the ground motion assessment and for four teams' methods and characterization models for the fault displacement assessment. The PSHA Calculations Team sent preliminary hazard curves and results of sensitivity analyses after the workshop to teams that did not complete their input in time to receive feedback at the workshop. At the end of the Feedback Workshop, a joint session was held with the SSFD experts and the GM experts. The purpose of this joint session was to provide an opportunity for interaction between the two groups of experts, specifically to discuss common issues, ask

questions about each other's interpretations and assessments, highlight any inconsistencies between the seismic source and ground motion characterizations, and come to a better common understanding of the linkages between the two groups' input to the seismic source and fault displacement. For example, a subject of considerable discussion was the geometry of seismogenic sources, especially interpretations that call for the simultaneous rupture of multiple Yucca Mountain faults. In addition, interpretations of earthquake stress drop were discussed. The summary of this workshop includes more detail on these and other issues discussed during the Feedback Workshop (Appendix C).

3.2.6 Workshop #6-Fault Displacement

The Fault Displacement Workshop, June 3, 1997, the final workshop conducted for the seismic source and fault displacement characterization, was designed to provide feedback to the teams on their fault displacement approaches and assessments. The threefold purpose of the 1-day workshop was to (1) review and discuss alternative methods and models for assessing fault displacement, (2) discuss uncertainties in parameter values and models, and (3) facilitate the expert teams' discussion of the pros and cons of alternative approaches, models, and submodels. Prior to the workshop, a "white paper" summarizing the fault displacement evaluation approaches developed by the expert teams was prepared by the SSFD Facilitation Team and distributed to the experts. During the workshop, the approaches taken by each expert team to evaluate displacement at nine demonstration points were reviewed in more detail than at the previous workshop. This was followed by extensive discussion and technical challenge about the strengths and weaknesses of all the approaches, data required to apply them, and uncertainties in model parameters.

The methods used for estimating the frequency of displacement events and the expected displacement per event at locations where faults or fractures are present in Tertiary rocks, but Quaternary paleoseismic data are lacking, were discussed extensively. Discussion also focused on the use of data from historical surface faulting events to develop relations for the likelihood of distributive faulting and the pros and cons of approaches using observed displacements versus those that rely on mechanical models of rock deformation. The experts explained different approaches to characterizing both along-strike and event-to-event variations in displacement. Presentations also were given on newly available information from the ESF, as the tunnel boring machine had completed its excavations since Workshop

#5. More details on these presentations and the fault displacement issues discussed are included in this workshop summary (Appendix C).

3.3 ELICITATION OF SSFD EXPERTS

The elicitation interviews involved a series of activities, which can be grouped into two steps: (1) preparation for the interviews and (2) the elicitation interviews.

3.3.1 Preparation for the Elicitation

Peter Morris of the SSFD Facilitation Team provided elicitation training at Workshop #4. The objectives of the training were to demonstrate how to quantify uncertainties using probabilities, to recognize common cognitive biases and compensate for them, and to present examples of the types of assessments that would be made at the elicitation interview (e.g., continuous variables, discrete hypotheses, and associated weights). The training was designed to help the experts be comfortable with the *process* of elicitation, so that the elicitation interview itself could focus on the *technical issues* of importance to the seismic source and fault displacement characterization.

At Workshop #4, the experts had been informed that the seismic source characterization issues presented would be covered in the elicitation interviews. A memo providing guidance for the characterization of fault displacement was provided to the expert teams before the elicitation interviews. The memo described the alternative approaches available to evaluate fault displacement (earthquake-based approaches that rely on the location, frequency, and size of earthquakes, and displacement-based approaches that evaluate the amount and frequency of displacement directly from displacement observations). In addition, the memo identified nine demonstration points within the Controlled Area that would serve as representative points (representing the range of expected conditions) at which all teams' fault displacement methodologies would have to be operative.

3.3.2 Elicitation Interviews

The elicitations of the expert teams took place in separate 1-day interviews in the San Francisco office of Geomatrix Consultants. The interviews were conducted by members of the SSFD Facilitation Team. Dr. Coppersmith (specialist and normative expert) and Dr.

Youngs (generalist and hazard analyst) attended all of the interviews, Dr. Perman, Ms. Olig, and Dr. Morris (normative expert) attended selected interviews. Drs. Whitney and Toro, and an NRC representative, also attended some interviews to observe the process followed.

All data sets provided or made available to the experts during the project were present during the elicitation. The elicitation interview followed a logical sequence from general to more specific assessments. Alternative models, approaches, and hypotheses were discussed, and the logic structure for the assessments and associated probability distributions were developed. Team members discussed the various issues among themselves and arrived at alternative models and probability distributions that they believed spanned the range of views across their team and across the larger technical community. The SSFD Facilitation Team representatives took written notes of all assessments during the interviews.

3.3.3 Documentation and Review

Documentation of the expert elicitations began with documentation and a summary prepared by the SSFD Facilitation Team representatives during the interviews. Experience on several other expert elicitation projects has shown this approach to be preferable to other documentation methods (e.g., written questionnaires, experts writing their interpretations following the interview, or tape recordings). During the 1-day interview, each expert team was asked to make many assessments, to quantify uncertainties, and to provide the technical bases for their interpretations. By having the SSFD Facilitation Team document and summarize, experts were free to focus on thinking through their answers and thoroughly expressing interpretations. The SSFD Facilitation Team was able to be flexible in the elicitation sequence (i.e., following the logic comfortable to the team) while ensuring that all elements were covered.

Following the interviews, the SSFD Facilitation Team provided each expert team with written documentation of the interview, organized by model component. The experts, in accordance with the requirements of the Project Plan, independently prepared a summary that reflected their interpretations. The summaries prepared by each expert team became the first draft document. This draft was reviewed for logical consistency and completeness and returned to the expert team for revision. The revised summary became a second draft that was reviewed by Dr. Stepp. These reviews were conducted to provide for completeness and

clarity of documentation. The teams responded to any requests for further clarifications, and the summaries were finalized. The elicitation summaries are provided in Appendix E.

3.3.4 Feedback and Sensitivity

Feedback to the experts occurred throughout the seismic source and fault displacement characterization, primarily through interaction among experts. By presenting their evaluations of models and associated interpretations at workshops and in general discussions, the experts both provided and received feedback from their peers on the panel.

More formally, feedback was provided to the experts using several approaches.

- At Workshop #4, the expert teams presented their preliminary interpretations regarding the key technical issues to the other teams. The teams were encouraged to understand the alternative views, their technical bases, and uncertainties.

- At Workshops #5 and #6, which occurred after the elicitation interviews, discussion focused on team interpretations. Discussions included the technical bases for the interpretations, the weights assigned to alternative hypotheses, and expressions of uncertainty in parameter values and alternative models (e.g., logic trees).

- Calculations showing the results of each team's initial interpretations were presented at Workshops #5 and #6. Calculations included maximum magnitude distributions, earthquake recurrence relationships for important seismic sources, calculated seismic hazard curves and dominant contributors, and fault displacement hazard curves and dominant contributors.

- Prior to the finalization of the seismic source and fault displacement models, each team was provided with (1) calculations showing the results of their preliminary interpretations, (2) plots showing the sensitivity of their results to alternative maximum magnitude and recurrence approaches or models, and (3) comparison of the calculated seismic hazard curves for all sources combined for all teams to mean recurrence estimates for individual teams. Conference calls with each of the

teams and members of the SSFD Facilitation Team were conducted to provide clarification and additional feedback. Revisions to the seismic source and fault displacement models based on the feedback provided were incorporated into the final results.

- Members of the SSFD Facilitation Team, Project Management Team, and Review Panel reviewed the written elicitation summaries for clarity, adequacy, and completeness of documentation of the technical basis for the evaluations described in them.

The feedback-revision process required the experts to defend/revise their assessments as considered appropriate and to provide appropriate documentation. In all cases, the experts responded positively to critical reviews of their documentation. The resulting assessments and finalized elicitation summaries reflect the significant effort expended by each expert team.

3.3.5 Aggregation of Expert Assessment

The approach taken to combine, or aggregate, the expert evaluations is equal weighting. This approach was not a default but a goal from the start of the project, a goal the experts were apprised of throughout the project. Accordingly, the proper conditions were created throughout the project to allow for using equal weights (SSHAC, 1997). The actions taken to provide these conditions included:

- Carefully selecting highly qualified experts who represent diverse disciplines and experience

- Establishing and confirming the commitment of each expert to provide the required effort throughout the project

- Identifying available data sets and disseminating them to all experts

- Educating the experts in issues important to seismic source and fault displacement characterization and training the experts in elicitation methodologies and the role of experts as evaluators

- Facilitating interaction among the experts in workshops and field trips to foster a free exchange of data and interpretations and scientific debate with respect to hypotheses and resolution of data

- Providing feedback and sensitivity analyses to the experts

- Providing an opportunity for experts to revise their assessments in light of feedback

It should be noted that, in accordance with the guidance provided by SSHAC (1997), conditions could have been such that different weights would have been necessary. For example, if an expert team had been unwilling or unable to devote the required time and effort to develop a complete assessment and documentation, that team would have been removed from the project.

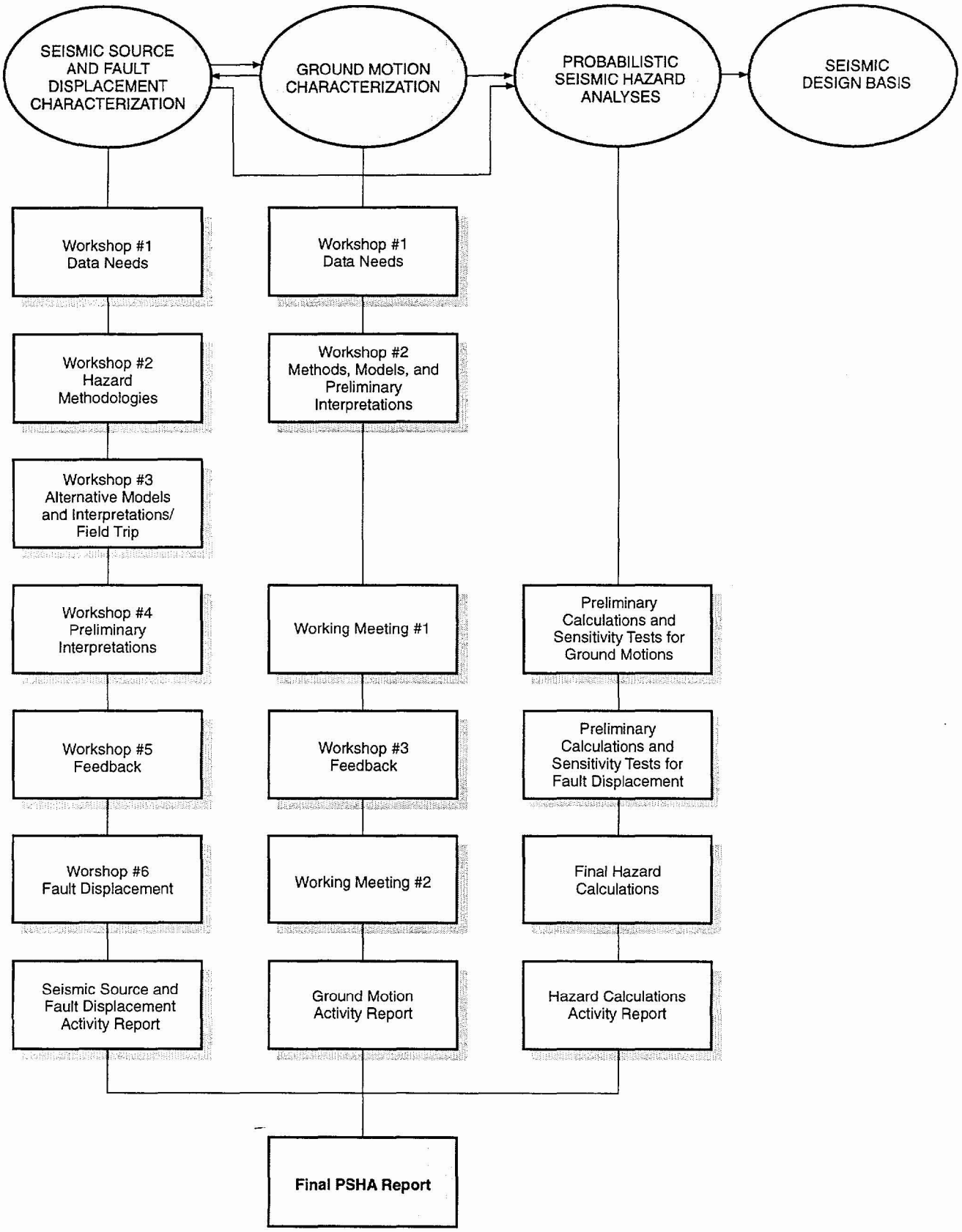

Figure 3-1 Probabilistic Seismic Hazard Analyses Project process for Yucca Mountain

4.0
SEISMIC SOURCE AND FAULT DISPLACEMENT CHARACTERIZATION

This section describes the methodologies used by the expert teams to (1) characterize the sources of potential earthquakes in the vicinity of the Yucca Mountain site for the PSHA for ground shaking hazard and (2) characterize fault displacement hazard within the Controlled Area. Section 4.1 presents the formulations used for seismic source characterization. Section 4.2 presents the formulations used for characterizing fault displacement hazard. The seismic source and fault displacement models developed by the six SSFD expert teams are described in Section 4.3. A detailed description of the PSHA methodology for vibratory ground motions is contained in Section 7.1.

4.1 SEISMIC SOURCE CHARACTERIZATION METHODOLOGY FOR GROUND MOTION HAZARD ASSESSMENT

The role of the SSFD expert teams in the ground motion PSHA is to identify the seismic sources that may produce earthquakes significant to ground motion hazard at the site. Then for each source they are to evaluate the frequency of earthquake occurrence, the maximum earthquake the source can produce, the distribution of earthquake sizes, and the spatial distribution of earthquakes on the source so that the distance to an earthquake of given magnitude can be computed. The methodologies used to assess these characteristics are discussed below.

4.1.1 Logic Trees

The PSHA methodology is formulated to represent the randomness inherent in the natural phenomena of earthquake generation and seismic wave propagation. The randomness in a physical process has come to be called *aleatory* uncertainty (SSHAC, 1997). In all assessments of the effects of rare phenomena, one faces uncertainty in selecting the appropriate models and model parameters because the data are limited and/or there are alternative interpretations of the data. This uncertainty in knowledge has come to be called *epistemic* uncertainty (SSHAC, 1997). The SSFD experts placed a major emphasis on developing a quantitative description of the epistemic uncertainty.

The uncertainty assessment was performed using the *logic tree* methodology. The logic tree formulation for seismic hazard analysis (Kulkarni *et al.*, 1984; Coppersmith and Youngs, 1986; EPRI, 1988; NRC, 1988) involves setting out the sequence of assessments that must be made in order to perform the analysis and then addressing the uncertainties in each assessment sequentially. Thus, it provides a convenient approach for dividing a large, complex assessment into a sequence of smaller, simpler components that can be addressed more easily.

Figure 4-1 shows an example of a logic tree. The logic tree is composed of a series of nodes and branches. Each node represents a state of nature or an input parameter that must be characterized to perform the analysis. Each branch leading from a node represents one possible alternative interpretation of the state of nature or parameter being evaluated. If the variable in question is continuous, it can be discretized at a suitable increment. The branches at each node are intended to represent mutually exclusive and collectively exhaustive states of the input parameter. In practice, a sufficient number of branches are placed at a given node to represent the evaluator's uncertainty in estimating the parameter.

Probabilities are assigned to each branch that represent the expert's evaluation that the branch represents the correct value or state of the input parameter. These probabilities are conditional on the assumption that all the branches leading to that node represent the true state of the preceding parameters. Because they are conditional probabilities for an assumed mutually exclusive and collectively exhaustive set of values, the sum of the conditional probabilities at each node is unity. The probabilities are based on scientific evaluations because the available data are often too limited to allow for objective statistical analysis, and because scientific evaluation is needed to weigh alternative interpretations of the available data. The logic tree simplifies these evaluations, because the uncertainty in each parameter is considered individually, conditional on assumed known states from prior evaluations. The nodes of the logic tree are sequenced to express conditional aspects or dependencies among the parameters and to provide a logical progression of evaluations from general to specific in characterizing the input parameters for PSHA.

The probabilities (relative weights) assigned to the branches at a node of the logic tree represent one of two types of probability assessments. For the first type, the branches at a node define the

range of parameter values; the associated weights define the probability distribution for the parameter. For example, estimates of the slip rate on a fault are uncertain because of uncertainties in the amount of displacement of a particular geologic unit across the fault and the age of the unit. The probability distribution for a parameter value may be characterized in several ways: as a discrete distribution defined by a preferred value and a range of discrete higher and lower values, a cumulative distribution based on scientific evaluations, or by a mean and standard deviation for a specified statistical distribution. Examples of these means of characterization are given below. Continuous distributions can be discretized to form logic tree branches following a number of approaches. Keefer and Bodily (1983) showed that most distributions can be represented reliably by three values: the median estimate (50^{th} percentile), assigned a weight of 0.63, and a higher and lower value, each given weights of 0.185, which represent the 5^{th} and 95^{th} percentiles (± 1.645 standard deviations for a normal distribution). They list other discretization schemes for more points. Another four-point representation of a normal distribution is described in EPRI (1993, Chapter 9). Miller and Rice (1983) present a number of discrete approximations to subjectively defined, continuous cumulative distributions.

In some instances, the uncertainty in assessing parameters can be estimated using formal statistical techniques. In these cases, continuous parameter distributions developed from statistical estimation procedures can be discretized for use in a logic tree formulation. An example of this approach is presented in Section 4.1.3.

A second type of probability assessment, to which logic trees are particularly well suited, is indicating a relative preference for, or degree of belief in, alternative hypotheses. For example, the sense of slip on a fault may be uncertain – two alternatives might be strike-slip or reverse-slip. Based on the pertinent data, a relative preference for these alternatives can be expressed by weights in the logic tree. A very strong preference (i.e., the data strongly support one interpretation over the other) for one alternative over the other usually is represented by weights such as 0.9 and 0.1. If there is no preference (i.e., the data equally support either alternative) for either hypothesis, they are assigned equal weights (0.5 and 0.5 for two hypotheses). Increasing the weight assigned to one alternative from 0.5 to 0.9 (or more) reflects increasing support in the data for that alternative. Because the relative weights ultimately are the result of scientific evaluations based on available information, it is important to document

the data and interpretations that led to the characterization of parameter values and their relative weights so that the process can be reviewed by others.

The example logic tree shown on Figure 4-1 characterizes the uncertainty in assessing the magnitude of paleoearthquakes that have occurred on a fault on the basis of dip-slip offsets observed in a trench placed across the fault. (Such assessments may be one means of characterizing the maximum magnitude [M_{max}] for a seismic source.) There may be multiple sources of uncertainty in the assessment. Stratigraphic relationships in the trench walls may be somewhat ambiguous so that the amount of dip-slip displacement can be estimated only within a factor of two (e.g., 1.0 to 2.0m). One may also be uncertain about the existence of a significant component of lateral slip, which would indicate whether the fault is primarily a normal fault or an oblique-normal fault having a ratio of strike slip to dip slip in the range of 1:1 to 1.5:1. In addition, there is the uncertainty in whether the observed slip is more representative of the maximum slip during the paleoearthquake or the average slip.

The logic tree expresses these uncertainties. The interpretations in the logic tree usually are ordered from general to specific (Figure 4-1). The order of the interpretations, however, is dictated primarily by convenience in dealing with interdependencies in the characterization. For example, the down-dip width of a fault is a function of the thickness of the seismogenic crust and the fault dip. While fault dip may differ from fault to fault in an area, the seismogenic thickness may be the same for all the faults. Therefore, it is more convenient to place the assessment of thickness before the assessment of dip. After the logic tree is constructed, the order of the nodes can be changed. In cases where the interpretation depends on the state of another unknown, then it is placed to the right of that one in the logic tree.

In the example on Figure 4-1, the total amount of fault offset is dependent on whether the fault is a normal fault or an oblique-normal fault. In addition, the evaluation of whether the observed displacement is representative of the maximum or the average displacement may also depend on the style of faulting. The trench may have been placed in an area where the fault scarp was most pronounced, indicative of maximum vertical displacement. However, this may not be the area of maximum slip if the fault is oblique-normal. Because these two interpretations are made more easily given knowledge of the style of faulting, the node for interpretations of the style of faulting is placed first (to the left) in the logic tree. For the example on Figure 4-1, the

evaluation of the assessor is that the interpretation of normal faulting is preferred slightly (0.6) to the interpretation of oblique-normal faulting (0.4). In actual interpretations, the assessor documents the reasons for this evaluation.

Further characterization in the example (Figure 4-1) addresses the amount of displacement. The stratigraphic relationships indicate from 1.0 to 2.0 m of offset. The interpretation of these data may favor displacements in the range of 1.0 to 1.5 m but allow for as much as 2.0 m. Thus, if the fault is a normal fault, the distribution for the observed offset may be specified by three discrete values: 1.0, 1.5, and 2.0 m. The probabilities (relative weights) assigned to these values are 0.4, 0.4, and 0.2, respectively, reflecting that the data more strongly support displacements of 1.0 to 1.5 m.

If the fault is considered an oblique-normal fault, then the observed offsets must be increased to account for unmeasured strike-slip offset to obtain the net slip on the fault plane. The factor of increase is 1.4 for a 1:1 strike-slip/dip-slip ratio, and 1.8 for a 1.5:1 strike-slip/dip-slip ratio. In this example, it is considered twice as likely that the strike-slip to dip-slip ratio is closer to 1:1 than to 1.5:1. Thus the factors are given relative weights of 0.67 and 0.33. The evaluation of the strike-slip to dip-slip ratio is added to the logic tree after the branch for oblique-normal faulting. The evaluation is unnecessary along the normal faulting branch. There the distributions for the amount of net slip are assumed to be equal to those developed for normal faulting multiplied by the appropriate factor.

The final evaluation is whether the observed offsets represent maximum displacements or average displacements. This evaluation is important because separate empirical relationships between magnitude and fault offset are given for maximum and average displacement (e.g., Wells and Coppersmith, 1994). (One could, of course, argue that other interpretations are possible in an exhaustive list of alternatives. It is important that the evaluator considers a sufficiently broad distribution of alternative interpretations to adequately represent the uncertainties in the assessment.) The evaluation of the relative likelihood of the two interpretations is made conditionally on which sense of slip is assumed to be correct—that is, the probability that the observed offset is a maximum given normal faulting is a separate evaluation from the probability that it is a maximum displacement given oblique-normal faulting, and the two probabilities do not have to be equal. In the example the data strongly

support the interpretation that the observed displacements represent maximum (0.8) rather than average (0.2) values if the style of faulting is deemed normal. If the fault is considered oblique-normal, then the maximum and average displacement is considered to be equivocal, and the two alternatives are given equal weight.

Each end branch on the right-hand side of the logic tree (Figure 4-1) specifies one estimate for the magnitude of the paleoearthquake. The magnitude estimate is obtained using the appropriate empirical relationship between fault displacement (either average or maximum) and moment magnitude (M_w) given by Wells and Coppersmith (1994). Their relationships for normal faulting earthquakes were used for the normal style of faulting; their relationships for strike-slip faulting were used for the oblique-normal style of faulting. The resulting magnitudes are listed along the right side of the logic tree. Each magnitude assessment listed on the right-hand side of the logic tree represents a specific set of states of the parameters, and the joint probability of that set is equal to the product of the conditional probabilities assigned to each branch. These probabilities are given in parentheses next to the magnitude assessments. It is possible that two or more end branches may result in the same magnitude estimate (within a specified tolerance), and the joint probabilities can be added together in forming a distribution for the assessed variable. These probabilities are given in parentheses next to the magnitude assessments. The characterization in the logic tree specifies a discrete distribution for the magnitude of the paleoearthquake. This distribution is shown at the right of Figure 4-1 in discrete density and cumulative forms.

The process illustrated above for characterizing magnitude of paleoearthquakes was used to quantitatively express the uncertainty in the seismic source characterization for ground shaking hazard. Each SSFD expert team identified potential seismic sources and then characterized their geometry, M_{max}, frequency of occurrence, and spatial distribution of earthquakes. The scientific uncertainty in all of these evaluations was expressed using the logic tree format. Although it is not necessary that all six teams adopt the same logic tree structure, it was suggested that similar forms be used to facilitate discussion between the teams of the important issues.

Figure 4-2 shows the general structure of a logic tree used to develop the seismic source model to represent faulting within the immediate vicinity of the Yucca Mountain site. The logic tree

begins on the left with consideration of the alternative tectonic/faulting models that may control the number and characteristics of the seismic sources that would be defined for the region. These alternative models may include planar faults extending through the seismogenic crust, a shallow detachment with planar faults above and perhaps a strike-slip source at depth, one or more master faults at depth with coupled surface faults at the surface, or some other model.
The second level of the logic tree expresses the uncertainty in the maximum depth of seismogenic rupture. This is important to the evaluation of M_{max} as well as earthquake recurrence based on fault slip rate .

The next two levels express alternative source configurations for each tectonic model. For example, given the planar fault model, one may have alternative interpretations as to which faults are independent and which faults are coupled. For the detachment model, there may be uncertainty about the depth of the detachment and the underlying driving mechanism. For the master fault, there may be uncertainties about the number of master faults and which of the surface faults are coupled at depth. There may be several levels at this point that express uncertainties in specific attributes of a tectonic/faulting model that are common to all of the seismic sources that will be defined using that model.

At this point, the logic tree lists the individual seismic sources defined by a given tectonic/faulting model and a specific set of model attributes. Here the logic tree branches into subtrees, one subtree for each identified seismic source. We use the convention of a vertical line connecting a series of seismic sources, each with is own subtree, to denote the summation of hazard from multiple sources. No dot is placed at the connecting point, indicating that these are not alternatives but individual, independent sources. The distributions of parameters for each source (defined by the subtree to the right of the source name) are assumed to be independent.

The next level of uncertainty expressed is the likelihood that an individual source is active, that it produces earthquakes in the current tectonic regime. If a source is active, then it is considered a discrete seismic source that contributes to the hazard.

The remaining levels of the logic tree characterize the evaluations of M_{max} and seismicity rate parameters. The approaches that may be used for these evaluations are discussed in Sections 4.1.3 and 4.1.4, respectively.

The logic tree structure shown on Figure 4-2 presents a general framework for representing the uncertainty in defining and characterizing the local seismic sources in the immediate vicinity of the Yucca Mountain block. In addition to these sources, the SSFD expert teams identified and characterized regional sources consisting of specific faults and areal zones of seismicity that cannot be attributed to specific known faults. Figures 4-3 and 4-4 present example logic tree structures used to represent the uncertainties in identifying and characterizing these two types of regional sources.

Figure 4-3 presents an example logic tree structure for the regional fault sources. The first level of the logic tree characterizes interpretations of alternative regional tectonic models that are considered to affect which regional faults are considered potential seismic sources. The logic tree is then expanded into subtrees for each of the individual faults or fault zones considered potential sources. The next level of the logic tree characterizes alternative interpretations of the coupling of individual faults within a particular fault zone or fault system. For example, the evaluator might consider the Furnace Creek and Death Valley faults to be part of a single fault system. They may be a single fault having one set of characteristics, or they may be two separate faults having independent characteristics. The remaining levels of the logic tree characterize the individual fault or fault segment activity, maximum seismogenic depth, M_{max}, and seismicity rate parameters.

Figure 4-4 presents an example logic tree structure for regional areal source zones. Areal source zones are sometimes referred to as "background" sources. Within the framework of this PSHA, areal source zones and background sources are equivalent. Both terms refer to a region where seismicity is not associated with specific geologic structures (faults), but instead is represented by a specified spatial distribution. The first node of the logic tree characterizes alternative approaches for zonation of the region. The alternatives may include defining areal source zones having a uniform spatial density of seismicity, defining areal source zones having a nonuniform spatial density of seismicity, or the spatial smoothing of seismicity without defining specific source zone boundaries. At this point, the logic tree is expanded into subtrees

for each areal source zone. The remaining levels of the logic tree characterize alternative parameters for defining the spatial distribution of seismicity within each zone or within the region, the M_{max}, and the seismicity rate parameters.

4.1.2 Types of Seismic Sources and the Spatial Distribution of Seismicity

Two types of seismic sources were used by the SSFD expert teams, faults and areal source zones. Fault sources are used to represent the occurrence of earthquakes along a known or suspected fault trace or traces. Uncertainty in the definition of fault sources is expressed by considering alternative total lengths, alternative fault dips, and possible linkages with other faults. In addition, an evaluation is made of the probability that a particular fault is active, i.e., the fault produces earthquakes in the current tectonic regime.

Faults were represented in the PSHA by segmented planar features; the fault dip and the minimum and maximum depths of rupture on the fault plane were specified by the SSFD expert teams. Earthquake ruptures typically are considered to occur with equal likelihood at any point on the fault plane, the size of the rupture being specified by an empirical relationship between magnitude and rupture area.

Areal sources represent areas of distributed seismicity that are not apparently associated with specific known faults and, therefore, are considered to be occurring on unidentified and/or unidentifiable faults. Areal source zones may also be used to model the occurrence of earthquakes at great distances from a site when the details of the individual faults are not significant to the hazard assessment. The boundaries of areal zones delineate areas that have relatively uniform seismic potential in terms of earthquake occurrence and maximum earthquake magnitude. Uncertainty in defining areal zones typically was expressed by considering alternative zonations of the region surrounding the Yucca Mountain site.

Two alternative approaches were used by the SSFD expert teams to characterize the spatial distribution of future earthquakes within the areal zones. The first considers that there is equal likelihood of occurrence of earthquakes at all locations within the zone. Under this interpretation the spatial density, $f(x,y)$, of future earthquakes at any point x,y in the areal zone is $1/A_Z$, where A_Z is the area.

The alternative interpretation was nonuniform spatial occurrence expressed by a nonuniform spatial density function for the areal zone using the recorded seismicity estimation of kernel density. This interpretation implies that future seismicity is more likely to occur near where it has in the historical past. This interpretation currently is being used to develop the national seismic hazard maps for the U.S. (Frankel, 1995).

The kernel density estimate of the spatial density function is given by the expression

$$f(x,y) = \frac{\sum_{i=1}^{N} K(d_i, h)}{\iint_Z \sum_{i=1}^{N} K(d_i, h) \cdot dx \cdot dy} \tag{4-1}$$

where $K(d_i,h)$ is a kernel density function with characteristic dimension h, and d_i is the distance from point x,y to the i^{th} earthquake in the source zone. The denominator in Equation (4-1) is the integral of the spatial density over the region of the areal zone; this normalizes the kernel density estimate to a proper probability density function.

The SSFD expert teams chose to use a two-dimensional Gaussian kernel function. The form of the kernel function is (Silverman, 1986)

$$K(d_i, h) = \frac{e^{-d_i^2/2h^2}}{2\pi h^2} \tag{4-2}$$

The controlling factor in kernel density estimation is the selection of the characteristic dimension h. The SSFD expert teams expressed the uncertainty in defining a nonuniform spatial density by considering various values for h.

4.1.3 Assessment of Maximum Magnitude

The M_{max} for a seismic source represents the largest earthquake for the source, regardless of its frequency of occurrence. Thus, M_{max} defines the upper limit of the earthquake recurrence relationship for the source.

4.1.3.1 Fault-Specific Sources. The approach used to evaluate the M_{max} for a fault source was to estimate the maximum physical dimensions of rupture on the source and use relationships between rupture dimensions and earthquake magnitude to estimate M_{max}. The types of empirical relationships available are magnitude versus rupture length, rupture area, maximum surface displacement, and average surface displacement. Some published empirical relationships include more than one parameter, such as rupture length and slip rate or the product of rupture length and displacement (e.g., Anderson *et al.*, 1996). Estimates of the rupture area and average slip on the fault can also be used to estimate the seismic moment of the maximum event, which then can be converted to M_w using the relationship specified by Hanks and Kanamori (1979). The PSHA was conducted using M_w as the magnitude measure, because this is the scale of choice in ground-motion estimation; all estimates of M_{max} were converted to this scale.

The SSFD expert teams considered multiple sources of uncertainty in estimating M_{max} for fault sources. These include consideration of the (1) relative merit of alternative rupture characteristics for estimating magnitude (such as estimates based on rupture length versus estimates based on maximum displacement), (2) relative merit of alternative published empirical relationships, and (3) uncertainty in estimating the physical dimensions of the maximum rupture on a fault. Figure 4-5 illustrates the approach used to express these uncertainties. In the example, alternative fault widths are assessed by considering a range of permissible maximum depths of rupture and alternative fault dips. Alternative maximum rupture lengths are assessed based on evidence for lasting segmentation points and differences in fault behavior. Alternative empirical relationships are considered: magnitude versus rupture length or rupture area from Wells and Coppersmith (1994), or magnitude versus rupture length and slip rate (Anderson *et al*, 1996). If the Anderson *et al.* (1996) relationship is used, then a distribution of possible fault slip rates is assessed. The example logic tree shown at the top of Figure 4-5 shows only some of the branches to illustrate the various evaluations. The complete logic tree leads to the discrete distribution for M_{max} shown at the bottom of the figure.

4.1.3.2 Areal Source Zones. Different approaches may be used to evaluate the M_{max} for areal zones. In cases where an areal zone is used to model the occurrence of earthquakes at large distances from a site where the details of the individual fault sources are not significant to the

hazard assessment, the M_{max} represents the largest earthquake determined to occur on any of the faults within the areal zone. In cases where areal zones are used to model the occurrence of earthquakes on unknown faults (there may be fault sources within the areal zone that are modeled explicitly as separate sources in the hazard), the M_{max} for the areal zone is determined by the largest fault within the zone that is mapped, or the largest earthquake that is not associated with surface faulting. The size of this fault will depend on the level of detailed mapping of the region and the identification of fault sources. Guidance for this evaluation is provided by studies that examine the frequency at which earthquakes of various magnitudes rupture the surface (e.g., Wells and Coppersmith, 1993; de Polo, 1994; and S. K. Pezzopane and T. E. Dawson, USGS, written communication, 1996). The data sets of de Polo (1994) and S. K. Pezzopane and T. E. Dawson (USGS, written communication, 1996) are specific to the Basin and Range Province.

4.1.4 Assessment of Earthquake Recurrence

Earthquake recurrence relationships for a seismic source describe the frequency at which earthquakes of various magnitudes occur. They are determined by estimating the overall frequency of earthquakes on the source, $\alpha_n(m^0)$, and the relative frequency of earthquakes of various sizes defined by the probability density of earthquake size, $f(m)$, between m^0 (minimum magnitude) and the upperbound magnitude, m^U. Different approaches were used to determine the recurrence relationships for areal source zones and fault sources.

4.1.4.1 Areal Source Zones. The earthquake recurrence relationships for areal zones were determined from the historical seismicity. Appendix G describes the development of the earthquake catalog for the region within 300 km of the Yucca Mountain site. The earthquakes in the catalog are described in terms of a uniform magnitude scale, M_w. The catalog was analyzed to identify dependent events (earthquakes that were aftershocks or foreshocks of larger earthquakes) to produce data sets of earthquakes that can be considered to correspond to a Poisson process. Several alternative methods for identifying dependent events were used to express the uncertainty in the process. The SSFD expert teams used the alternative catalogs (as discussed in Appendix G) to develop alternative recurrence relationships for their areal source zones.

The distribution of earthquake sizes in each areal zone was interpreted to follow the Gutenberg and Richter (1954) exponential recurrence model. Because each source has a defined M_{max}, the truncated exponential magnitude distribution (Cornell and Van Marke, 1969) was used to define the recurrence relationships. The truncated exponential relationship is of the form

$$N(m) = \alpha(m^0)\frac{10^{-b(m-m^0)} - 10^{-b(m^U-m^0)}}{1-10^{-b(m^U-m^0)}} \tag{4-3}$$

where $N(m)$ is the annual frequency of occurrence of earthquakes of magnitude greater than m, and b is the Gutenberg and Richter (1954, 1956) b-value parameter.

The recurrence parameters needed for each areal zone are $\alpha(m^0)$ and b. The maximum likelihood procedure developed by Weichert (1980) was used to estimate these parameters from the historical catalog. The likelihood function used in this study was modified from that presented by Weichert (1980) to allow for variable periods of complete reporting within the boundaries of the source as well as variable magnitude intervals (Johnston *et al.*, 1994). The source zone is divided into subregions in which the catalog is considered to be homogeneous. The procedure then sorts the catalog by size into a number of magnitude intervals of width Δm. For each magnitude interval, $m_i \leq m < m_i+\Delta m$, and for each of the j subregions of the source, the period of complete reporting, t_{ij}, is identified. Given the truncated exponential recurrence model, the expected frequency of occurrence of earthquakes of magnitude $m_i \leq m < m_i+\Delta m$ within the j^{th} subregion is defined as $\lambda_j(m_i)$ and is given by the expression

$$\lambda_j(m_i) = \alpha(m^0)\frac{e^{-\beta(m_i-m^0)} - e^{-\beta(m_i+\Delta m-m^0)}}{1-e^{-\beta(m^U-m^0)}} \cdot A_j / A_Z \tag{4-4}$$

where $\beta = b \cong \ln(10)$, A_j is the area of the j^{th} subregion, and A_Z is the total area of the source zone. Interpreting the occurrence of earthquakes within the source to be described by a Poisson process, then the likelihood of observing the recorded catalog is given by

$$L\{\alpha(m^0),\beta\} = \prod_i \prod_j \frac{[\lambda_j(m_i)t_{ij}]^{k_{ij}} e^{-\lambda_j(m_i)t_{ij}}}{k_{ij}!} \quad (4\text{-}5)$$

where k_{ij} is the number of earthquakes of magnitude $m_i \leq m < m_i+\Delta m$ that have been recorded in the j^{th} subregion during the period of compete reporting t_{ij}. The maximum likelihood recurrence parameters for the source are found by maximizing L{ $\alpha(m^0)$, β }over $\alpha(m^0)$ and β.

The uncertainty in the recurrence relationships for the regional sources was characterized as follows. Using the asymptotic standard errors in $\alpha(m^0)$ and β computed from the maximum likelihood fit to the data, five values of $a(m^0)$ and five values of b were defined ranging from -2 standard deviations to +2 standard deviations. These were then used to define 25 recurrence relationships (Figure 4-6) that may have generated the observed data. The likelihood that the observed data were a product of the process defined by each of the recurrence relationships was computed using Equation (4-6). These likelihoods were then normalized to define a discrete distribution for the seismicity parameters. The resulting distribution indicates the degree to which the data constrain the recurrence relationship for the source zone and accounts for the correlation between $\alpha(m^0)$ and β. Figure 4-6 shows an example of the resulting distribution in computed earthquake recurrence frequencies, including the uncertainty in M_{max}. An additional level of uncertainty in the recurrence relationship for the areal source zones was consideration of the alternative catalogs of independent earthquakes generated using the alternative declustering methods.

4.1.4.2 Fault-Specific Sources. Two approaches were used to estimate the earthquake recurrence relationships for faults. The first involved estimating the frequency of large-magnitude surface-rupturing earthquakes on the fault either by dating of paleoearthquakes or by dividing an estimate of the fault slip rate by an estimate of the average slip per event. The complete recurrence relationship for the source is then specified by constraining a particular form of an earthquake recurrence model (magnitude distribution function) to pass through the estimated frequency of large events. The second approach was to translate the estimated fault slip rate into seismic moment rate and then partition the moment into earthquakes of various magnitudes according to the magnitude distribution or recurrence model used. Both of these approaches constrain the earthquake recurrence relationship for the fault at the frequency of

magnitudes near the M_{max}. The frequency of smaller-magnitude earthquakes is then extrapolated from this frequency based on the form of the magnitude distribution used.

Several magnitude distribution models were considered by the SSFD expert teams (Figure 4-7). One form is the "characteristic" earthquake magnitude distribution developed by Youngs and Coppersmith (1985). The form of the characteristic magnitude distribution is

$$N(m) = N^e \frac{10^{-b(m-m^O)} - 10^{-b(m^U-\frac{1}{2}-m^O)}}{1-10^{-b(m^U-\frac{1}{2}-m^O)}} + N^C \quad for\ m^O \le m < m^U - \frac{1}{2} \qquad (4\text{-}6)$$

$$N(m) = N^C \frac{m^U - m}{\frac{1}{2}} \quad for\ m^U - \frac{1}{2} \le m < m^U$$

with $$N^e = N^C \frac{1.0 - 10^{-b(m^U-1-m^O)}}{\frac{1}{2} b \ln(10) 10^b 10^{-b(m^U-1-m^O)}}$$

where the terms N^e and N^c represent the rate of exponential and characteristic events, respectively. $N^c = N(m^U\text{-}½)$, the cumulative frequency of characteristic events, and the total seismicity rate equals the sum of the rate for exponential and characteristic events, $\alpha(m^0) = N^e + N^c$. When the rate of large events is specified by the SSFD expert teams, it is assumed to be equal to N^c, and Equation (4-6) is used to define the recurrence relationship. When the recurrence relationship is to be based on slip rate, then the parameters N^e and N^c are given by

$$N^e = \frac{\mu A_f S \left[1 - 10^{-b(m^U-\frac{1}{2}-m^O)}\right]}{M_O(m^U) 10^{-b(m^U-\frac{1}{2}-m^O)} \left[\frac{b \cdot 10^{\frac{-c}{2}}}{c-b} + \frac{b \cdot 10 b(1-10^{\frac{-c}{2}})}{c}\right]} \qquad (4\text{-}7)$$

$$N^C = \frac{\frac{1}{2} b \ln(10) N^e 10^{-b(m^U - \frac{3}{2} - m^O)}}{1 - 10^{-b(m^U - \frac{1}{2} - m^O)}}$$

where μ is the shear modulus of fault zone rock (taken to be 3×10^{11} dyne/cm^2), A_f is the total fault surface area, S is the slip rate, and $M_o(m^U)$ is the seismic moment for the m^U on the fault [$M_o(m)=10^{cm+d}$, with c equal to 1.5 and d equal to 16.1, Hanks and Kanamori (1979)].

The second recurrence model used was the truncated exponential model, Equation (4-3). When the recurrence for the fault is specified to be the recurrence interval for large events, it is interpreted to correspond to the frequency for earthquakes of m^U-½ , $N(m^U$-½), and Equation (4-3) is used to define the recurrence relationship for the source. When the recurrence relationship is to be based on slip rate, then the formulation developed by Anderson (1979) is used:

$$\alpha(m^O) = \frac{(c-b)\mu A_f S[1-10^{-b(m^U-m^O)}]}{b M_O(m^U) 10^{-b(m^U-m^O)}} \qquad (4\text{-}8)$$

Youngs *et al.* (1987) introduced a modification to the standard truncated exponential distribution that was used by one of the SSFD expert teams. The modification considers the upperbound magnitude in the density function to be uniformly distributed over the range of m^U-½ to m^U in a similar fashion to the characteristic earthquake model. The effect is to generalize the upper boundary of the magnitude distribution without altering the general shape of the recurrence relationship. The formulation for the modified truncated exponential is:

$$N(m) = \alpha(m^O)\left[1 - \frac{\left[1-10^{-b(m-m^O)}\right] - \left[\ln(f^U) - \ln(f^i)\right]}{b \cdot \ln(10)/2} \; for\; m^O \le m < m^U - \frac{1}{2}\right] \qquad (4\text{-}9)$$

$$N(m) = \alpha(m^O)\left[1 - \frac{\left[1-10^{-b(m-m^O)}\right]\left[\ln(f^U)-\ln(f^i)\right]}{b\cdot\ln(10)/2} - 2(m-m^U)\right] \text{ for } m^U - \frac{1}{2} \le m < m^U$$

$$f^i = 10^{b(m^U-\frac{1}{2})} - 10^{bm^O}$$

$$f^u = 10^{bm^U} - 10^{bm^O}$$

$$f^i = 10^{bm} - 10^{bm^O}$$

If the recurrence relationship for a fault is specified by the frequency of large earthquakes, then it is interpreted to equal the cumulative frequency for earthquakes of magnitude m^U-½, $N(m^U$-½), and Equation (4-9) is used to determine the recurrence relationship for the source. If the recurrence relationship is based on slip rate, then the integral of the event frequency derived from Equation (4-9) times the moment for each event is set equal to the moment rate. As a result, $\alpha(m^0)$ is given by

$$\alpha(m^O) = \frac{6\mu A_f S(c-b)}{\frac{M_o(m^U-\frac{1}{2})}{10^{b(m^U-\frac{1}{2}-m^O)}-1} + \frac{4M_o(m^U-\frac{1}{4})}{10^{b(m^U-\frac{1}{4}-m^O)}-1} + \frac{M_o(m^U)}{10^{b(m^U-m^O)}-1}} \quad (4\text{-}10)$$

The fourth magnitude distribution model the SSFD expert teams considered is the maximum moment model developed by Wesnousky *et al.* (1983), in which only large earthquakes are assumed to occur on the fault. For this model, the recurrence relationships were specified using Equations (4-6) and (4-7) for the characteristic model with N^e set equal to zero (no exponentially distributed events).

Figure 4-7 compares the shape of the exponential, modified exponential, characteristic, and maximum M_w distributions. Shown on the left are the four distributions developed for an assessed fault m^U of M_w 7.5, with the frequency of events larger than M_w 7 set at one per 5000

years. Shown on the right on Figure 4-7 are the magnitude distributions developed on the basis of a slip rate of 1 mm/yr and a fault area of 1,000 km^2. All the recurrence relationships were developed with a *b*-value of 0.8. As can be seen, the modified truncated exponential distribution is very similar to the truncated exponential distribution. The characteristic magnitude distribution results in about a factor of ten reduction in the frequency of small-magnitude events compared to the exponential model.

Uncertainty in the recurrence relationships for the faults can incorporate alternative recurrence models, alternative methods to constrain the rate of large events (i.e., slip rate versus recurrence interval), uncertainty in the slip rates and recurrence intervals, and alternative *b*-values.

4.2 METHODOLOGY FOR FAULT DISPLACEMENT HAZARD CHARACTERIZATION

At the present time, methodologies for the probabilistic assessment of fault displacement hazard (especially distributed faulting hazard) have not matured to the level of those used for the assessment of ground shaking hazard and there is little relevant literature. As a result, the SSFD expert teams developed a number of original approaches as part of their assessments for the project. These approaches were originated to a significant degree by one of the teams, were discussed in Workshops #4, #5, and #6, and then were refined and modified in the individual team characterizations of fault displacement hazard. The methods are based primarily on empirical observations of the pattern of faulting during earthquakes and on data gathered during studies of the faulting in the Yucca Mountain region. As part of these characterizations, the individual teams developed a number of empirical distributions from data gathered at Yucca Mountain or published in the literature. The SSFD Facilitation Team fit statistical models to these empirical distributions to facilitate numerical calculation of the hazard. Appendix H documents the development of these statistical models.

4.2.1 Principal and Distributed Fault Displacement

The potential for fault rupture within the Controlled Area can be described in terms of two types of fault rupture: *principal faulting* and *distributed faulting*. These are illustrated on Figure 4-8, which shows the surface rupture pattern for the 1959 M_W 7.4 Hebgen Lake earthquake. Principal faulting is the faulting along the main plane (or planes) of crustal weakness

responsible for the release of seismic energy during the earthquake. Where the principal fault rupture extends to the surface, it may be represented by displacement along a single narrow trace or over a zone that is a few to many meters wide. For principal faulting, the faults of concern are those that may produce earthquakes (i.e., are directly related to the primary source of energy release). Repeated large earthquakes on a given fault segment are considered to be produced by repeated principal faulting on the same fault trace or traces, so that faults that are capable of principal rupture can be recognized based on detailed mapping of outcrops and/or in the walls of subsurface excavations (trenches and tunnels).

Distributed faulting is defined as rupture that occurs on other faults in the vicinity of the principal rupture in response to the principal displacement. It is expected that distributed faulting will be discontinuous in nature and occur over a zone that may extend outward several tens of meters to many kilometers from the principal rupture. A fault that can produce principal rupture may also undergo distributed faulting in response to principal rupture on other faults. The extent to which faults that can undergo distributed rupture can be identified depends on the level of detailed mapping but the minimum resolution for detection is generally smaller for distributive faulting than for principal faulting. Interpretation of distributive faulting is more subjective and is, therefore, less certain than for principal faulting.

Both types of faulting are important to the assessment of the fault displacement hazard at the Yucca Mountain site. Figure 4-9 shows the Controlled Area and the nine locations at which the fault displacement methodology is demonstrated. These points were chosen to represent the range of conditions in the Controlled Area. Some of these points lie on faults that may experience principal faulting (the Solitario Canyon fault, the Bow Ridge fault, and possibly some of the intrablock faults) and distributed faulting. The other points are sites of potential distributed faulting. The locations and specific conditions for the nine points are described further in Section 4.3.2. The methodologies described below were developed by the SSFD expert teams to assess the hazard at any location within the Controlled Area, including all of these nine demonstration points.

4.2.2 Basic Formulation

The basic formulation for probabilistic evaluation of the hazard from fault displacement is analogous to that developed for the hazard from ground shaking. The fault displacement PSHA

addresses how frequently it occurs and how large the displacements are. The hazard can be represented probabilistically by a displacement hazard curve that is analogous to ground motion hazard curves. The hazard curve shown on Figure 4-10 represents the hazard at a point within the Controlled Area. It relates the amount of displacement in a *single* event to how often larger displacements occur (i.e., the frequency of exceeding a specified amount of displacement). In the example hazard curve (Figure 4-10), single event displacements larger than 10 cm occur with a frequency of 10^{-4} per year (a return period of 10,000 years); single event displacements larger than 50 cm occur with a frequency of 10^{-5} per year (a return period of 100,000 years). Thus, the hazard curve is a plot of the frequency of exceeding fault displacement value d, designated by $\nu(d)$. This frequency can be computed by the expression:

$$\nu(d) = \lambda_{DE} \cdot P(D > d) \tag{4-11}$$

where λ_{DE} is the frequency at which displacement events occur on the structure located at the point of interest, and $P(D>d)$ is the conditional probability that the displacement in a single event will exceed value d. The SSFD expert teams used different approaches to characterize fault displacement hazard and, thus, different techniques to express these two terms. They also used a variety of data sets to develop the necessary parameters. These approaches and data sets are generally described below. Specific applications of these approaches by each team are described in Section 4.3.2.

The displacement hazard curve can be used to estimate the effective slip rate on the feature of interest. The negative of the slope of the hazard curve, $\partial\, \nu(d)/\partial\, d$, provides the rate density of displacements of amount d. Integrating this over displacement provides an estimate of fault slip rate, SR. Specifically:

$$SR = \int_0^\infty \left[-\partial \nu(d) \Big/ \partial d \times d \right] dd \tag{4-12}$$

4.2.3 Assessment of Scientific Uncertainty

As with the ground motion PSHA methodology, the formulation given by Equation (4-11) represents the randomness in the natural phenomena of earthquake-induced fault displacement

(the aleatory uncertainty). The scientific (epistemic) uncertainty is represented in the process of selecting the appropriate models and model parameters for the fault displacement hazard characterization. The logic tree methodology described in Section 4.1.1 was utilized to characterize the uncertainty in the fault displacement PSHA.

4.2.4 Estimation of Displacement Event Frequency

The approaches for estimating the frequency of displacement events, λ_{DE}, developed by the SSFD expert teams can be divided into two categories. The first, designated the *displacement approach*, provides an estimate of the frequency of displacement events directly from observed feature-specific or point-specific data. The second, designated the *earthquake approach*, involves relating the frequency of slip events to the frequency of earthquakes on the various seismic sources defined by the seismic source characterization models developed in Section 4.3.1. Both approaches are used for assessing the fault displacement hazard for principal faulting and distributed faulting.

4.2.4.1 Displacement Approach. The displacement approach estimates the frequency of displacement events, λ_{DE}, from the information available for the specific feature (point) in question. There are two techniques for direct estimation of λ_{DE}, estimation of recurrence intervals and the use of slip rates.

Recurrence Interval Technique. An example of the recurrence interval technique is the assessment of the frequency of displacement events on a source of principal faulting using paleoearthquake data. The SSFD expert teams used such data to estimate the frequency of surface-rupturing events as part of their seismic source characterization models for the ground shaking hazard. This assessment can be used directly in assessing the frequency of faulting events.

Slip-Rate Technique. Fault slip rate, SR, is a measure of the amount of slip averaged over a time period that encompasses multiple ruptures. If the slip rate and the average slip in a faulting event, $\bar{D}_E$, are known, then λ_{DE} can be estimated by:

$$\lambda_{DE} = SR / \bar{D}_E \qquad (4\text{-}13)$$

Given *SR*, the use of Equation (4-13) requires an estimate of the average slip in an event, $\overline{D}_E$. For some features (typically those that may be the location of principal faulting), this may be assessed directly from trenching data. For other features, the SSFD expert teams developed scaling relationships that relate $\overline{D}_E$ to fault length, L, or cumulative fault displacement, D_{cum}. These are described in the summaries of the models the SSFD expert teams developed for displacement hazard (Section 4.3.2).

The displacement approach does not tie slip events to specific earthquakes, it only evaluates the frequency of slip events. Thus, the displacement approach does not explicitly distinguish between principal and distributed ruptures on a feature.

4.2.4.2 Earthquake Approach. The earthquake approach utilizes the earthquake recurrence models developed for the ground shaking hazard assessment. Each SSFD expert team provided an assessment of the frequency of earthquakes on each seismic source. The occurrence of a slip event (earthquake) on source j may induce slip on the feature (point) of interest, point i. The probability that slip will occur given an event on source j, P_i *(Slip| Event on j)*, can range from 0 to 1.0. The frequency of displacement events at point i, λ_{DE}, is obtained by summing the contributions from all of the seismic sources:

$$\lambda_{DE} = \sum_{j=i}^{n} \lambda_j \,(\text{Events on source } j) \cdot P_i\,(\text{Slip} \mid \text{Event on source } j) \qquad (4\text{-}14)$$

As defined by Equation (4-14), the earthquake approach for assessing the frequency of displacement events consists of two-parts, an evaluation of the opportunity frequency, the frequency of earthquakes, and an evaluation of the probability each opportunity will result in fault slip. Because the earthquake approach is tied directly to the occurrence of earthquakes on various sources, the distinction between principal and distributed faulting events is maintained.

The methods used to evaluate P_i *(Slip/ Event on j)* depend on whether one is considering principal ($j = i$) or distributed faulting ($j \neq i$).

Probability of Slip for Principal Faulting. In this approach the frequency of principal faulting events is assessed using earthquake recurrence models developed for a seismic source. The models define the frequency of various size earthquakes up to the maximum earthquake assessed for the source. In many cases, the recurrence models were developed by specifying the frequency of surface-rupturing earthquakes from trenching data, interpreting these events to be near the maximum earthquake. For these events, P_i *(Slip| Event on i)* is expected to be 1.0. However, earthquakes smaller than the maximum earthquake may not always rupture to the surface or at shallow depths where the repository is to be located (300 m). They also may have rupture lengths that are shorter than the total fault length. The contribution of these events to the fault displacement hazard will depend on their relative frequency compared to the largest events and the likelihood that they will rupture to near the surface and at the point along the fault where the hazard is being evaluated. Two approaches were developed to assess the probability of surface rupture in a principal faulting event, one based on empirical data on the frequency of surface rupture, and one based on the numerical randomization of the depth of rupture on the fault used in the analysis of ground shaking hazard.

Empirical Probability of Principal Faulting Surface Rupture. Wells and Coppersmith (1993), de Polo (1994), and S. K. Pezzopane and T. E. Dawson (USGS, written communication, 1996) present data sets that indicate the frequency at which earthquakes of various magnitudes rupture the surface. The data sets of de Polo (1994) and S. K. Pezzopane and T. E. Dawson (USGS, written communication,. 1996) are specific to the Basin and Range Province. These data can be used to develop an empirical model for P_i *(Slip| Event on i)* as a function of magnitude. For example, Wells and Coppersmith (1993) used a *logistic regression* model to evaluate the probability of surface rupture. The logistic regression model (e.g., Hosmer and Lemeshow, 1989) is a commonly used model for assessing the outcome of a dichotomous variable; in this case, surface rupture either occurs or does not occur. The probability of a positive outcome (the occurrence of principal faulting given the occurrence of the event) is given by the expression

$$P(\text{Rupture}) = \frac{e^{a+bm}}{1+e^{a+bm}} \tag{4-15}$$

where a and b are constants estimated from data (see Appendix H, Section H4.1). Figure 4-11 presents the results of fitting Equation (4-15) to the various data sets presented by S. K.

Pezzopane and T. E. Dawson (USGS, written communication, 1996) for surface rupture as a function of magnitude.

Focal Depth Distribution. Each SSFD team provided an evaluation of the focal depth distribution for earthquakes in the Yucca Mountain region. Using this distribution along with an assessment of the size of earthquake ruptures as a function of magnitude (e.g., an empirical relationship of rupture area as a function of magnitude) and rupture aspect ratio, the distribution for the down-dip location ruptures on a fault was modeled as part of the calculation of the source-to-site distribution in the ground motion hazard analysis. This process can also be used to calculate the frequency at which earthquakes of a given magnitude occurring on a fault are expected to rupture near the surface, thus providing a fault-specific estimate of P (*surface rupture*).

Probability of Intersection Along Strike. The probability that the earthquake rupture will intersect the point of interest along the fault is computed from the distribution for the location of the rupture along the fault. This distribution is computed for each fault as a part of the ground motion hazard assessment by assuming that earthquake ruptures are equally likely to occur anywhere along the fault. The probability of along-strike intersection of the rupture, $P(intersection)$, times the probability of surface rupture provides the probability of principal faulting in the earthquake, that is:

$$P_i(principal\ faulting\ slip | event\ on\ j) = P(surface\ rupture) \times P(intersection) \qquad (4\text{-}16)$$

Probability of Slip for Distributed Faulting. For distributed faulting, P_i (*Slip| Event on j*) expresses the likelihood that slip on an earthquake source some distance r from the feature of interest will trigger slip locally. Several approaches were considered for assessing P_i (*Slip| Event on j*) for distributed faulting.

Analysis of Historical Distributed Ruptures. S. K. Pezzopane and T. E. Dawson (USGS, written communication, 1996) developed a data base of distributed ruptures resulting from historical earthquakes in the western U.S. These data were used to assess the density of distributed ruptures as a function of distance from the principal rupture. The process used was to place a 0.5 km × 0.5 km grid on each map of surface ruptures. The number of grid cells that

contain a secondary rupture divided by the total number of grid cells at a given distance from the principal rupture provides a measure of the frequency or likelihood that a distributed rupture will occur. Figure 4-12 shows a plot of these data segregated by magnitude and by location in the hanging wall block and footwall block of the rupture. The data show a decrease in the likelihood of experiencing distributed rupture with increasing distance from the principal rupture. The data also show clear differences between the hanging wall and footwall sides of the rupture. The size (magnitude) of the earthquake appears to provide some control on the maximum distance distributed rupture has been observed away from the principal faulting.

The probability of occurrence of distributed faulting on a feature located r km from a magnitude m earthquake can be determined from these data using the logistic model.

$$P_i \text{ (Slip | Event on } j) = \frac{e^{f(m,r)}}{1+e^{f(m,r)}} \qquad (4\text{-}17)$$

where $f(m,r)$ represents a suitable function of m and r. The data shown on Figure 4-12 indicate that $f(m,r)$ should account for the effect of being on the hanging wall or foot wall sides of the principal rupture. Appendix H, Section H4.2 presents models fit to these data that were used by the expert teams to assess P_i (*Slip| Event on j*) for distributed faulting. This probability is considered an aleatory probability because it defines the likelihood of the occurrence of distributed faulting at a point in a single earthquake.

Slip Tendency. Another approach to estimating the likelihood that a feature will experience distributed faulting is based on characteristics such as feature and orientation. Morris *et al.* (1996) and H. L. McKague *et al.* (CNWRA, written communication, 1996) have performed slip-tendency analyses of faults in the Yucca Mountain region using their orientations with respect to the current stress field. These assessments have been used to either modify P_i (*Slip| Event on j*) (i.e., reduce the probability that distributed slip will occur as the orientation of the feature changes from favorable to unfavorable in the present stress regime) or as an assessment of whether the feature can slip at all in response to earthquakes in the present tectonic stress regime.

Another approach to assessing the likelihood that distributed slip could occur on a feature in response to principal faulting on a seismic source involves evaluating the angle between the strike of the principal fault and the strike of the feature under consideration. Section H4.3 of Appendix H presents an analysis of the pattern of distributed ruptures from mapping data developed by S. K. Pezzopane and T. E. Dawson (USGS, written communication, 1996). The relative frequency of rupture orientations with respect to the principal rupture provides an estimate of the likelihood that the feature will slip in response to a principal rupture.

4.2.5 Conditional Probability of Exceedance for Displacement

The conditional probability of exceedance, $P(D>d)$, in Equation 4-11, defines the probability that the amount of displacement occurring at a point during a single displacement event will exceed a specified amount d. The probability can be considered to contain two-parts: the variability of slip from event to event, and the variability of slip along strike during a single event. The first part represents a distribution for the "size" of faulting events and is analogous to an earthquake magnitude distribution model used in the ground shaking hazard analysis. The second part represents the variation of the displacement at a point from the size of the event. This might be considered analogous to the lognormal distribution for peak ground motion about the median value predicted by an attenuation law for a specific magnitude and distance.

The teams developed a variety of approaches for evaluating the distribution of slip at a point in an individual event. Some methods utilize the two-part representation of displacement variability; others combine them into a single distribution function. The various methods are described below as they are applied to principal and distributed faulting. The approaches also differ depending on whether the earthquake or displacement approaches are being used for the assessment.

4.2.5.1 Two-Step Approach for Conditional Probability of Exceedance. The two-part approach for assessing $P(D>d)$ was typically used in the earthquake approach for principal faulting hazard. The size measure used to describe the event was the maximum displacement, MD, in an earthquake and was typically assessed using empirical relationships between magnitude and maximum displacement. The value of MD in an event was assumed to be distributed according to the empirical regression model, typically lognormal. In some cases, the SSFD expert teams used trenching data to assess MD for maximum events on the source.

The second part is an assessment of the variability of slip at a point as a fraction of the maximum displacement in the event. The ASM team analyzed the slip distributions for a number of surface rupturing events. The plot on the left side of Figure 4-13 shows the results in the form of smoothed curves defining the minimum, median, and maximum values of *D/MD* at a point as a function of location along strike. These values, which can be interpreted as representing a low percentile, the median value, and a high percentile for *D/MD*, can be used to construct a cumulative distribution function for *D/MD*. Shown at the right of Figure 4-13 are examples of cumulative distribution functions for *D/MD* at three values of *x/L*, the location of the point along the rupture. These cumulative functions were made by fitting a beta distribution to the percentiles shown by the solid dots on the plot. The beta distribution was selected because it is a very flexible distribution for modeling variables that are defined over a finite range, in this case $0 \le D/MD \le 1$. The beta distribution has the density function

$$f(y) = y^{a-1}(1-y)^{b-1}\frac{\Gamma(a+b)}{\Gamma(a)\Gamma(b)} \tag{4-18}$$

where $\Gamma(\ )$ is the Gamma function. For this application, $y = D/MD$. The cumulative distributions shown on the right of Figure 4-13 were obtained by developing relationships for the parameters a and b as a function of x/L (see Appendix H). The SBK team developed a similar model for the distribution of *D/MD* using numerical simulations of fault rupture patterns (see Appendix H and the SBK elicitation summary in Appendix E).

The conditional probability of exceedance, $P(D>d)$, is then obtained by convolving the distribution for *D/MD* with the distribution for *MD* as a function of the magnitude of the earthquake.

$$P(D > d) = 1 - \int f(MD)\left[\int_0^{d/MD} f(y)\,dy\right] d(MD) \tag{4-19}$$

where $f(MD)$ was typically defined by a lognormal distribution and $f(y)$ is given by Equation (4-18).

4.2.5.2 Single-Step Approach for Conditional Probability of Exceedance. The single step approach for assessing $P(D>d)$ involved developing an empirical distribution for the displacement data collected at Yucca Mountain by normalizing the data from each trench location by a normalizing parameter related to the location where the data were obtained. The resulting distribution of D/D_{norm} were then used to compute $P(D>d)$, given an assessment for D_{norm} at the location of interest. A variety of normalization parameters were developed by the SSFD expert teams, including: the average displacement observed in a trench with multiple displacements, the average or maximum displacement expected for a fault based on its dimension, and the cumulative displacement that has occurred on the feature where the trench was located. These empirical distributions were then fit with statistical models for use in the displacement hazard computation (see Appendix H). Examples of these distributions are shown on Figure 4-14.

4.3 EXPERT TEAM MODELS

The following summarizes the expert team's seismic source characterization and a description of the fault displacement models. Complete expert team elicitation summaries are contained in Appendix E.

4.3.1 Seismic Source Characterization

The previous section describes the type of probabilistic models used to define the spatial location, frequency, and size distribution of earthquakes in the Yucca Mountain region that may generate significant ground motion at the repository. This section describes the seismic source models developed by the SSFD expert teams. Section 4.3.1.1 provides summaries of the individual team models, which are presented in full in each team's elicitation summary in Appendix E. This discussion is followed by a summary in which the assessments of key components of the source characterization models are compared (Section 4.3.1.2).

4.3.1.1 Individual Expert Team Models. The seismic source characterization models for each of the six SSFD teams are summarized in this section using common terminology and format. We do not attempt to summarize the bases for the teams' models, that information is contained in Appendix E. An abbreviated summary of models is given in Table 4-1. Lists of

acronyms used to designate fault sources on various source maps referred to in the following sections are given in Table 4-2. The seismic source characterization developed by each SSFD team is described in terms of local faults in the Yucca Mountain region, regional faults within 100 km of the site, and regional areal source zones. Much of the seismic hazard characterization involves assessing seismicity rates and M_{max} for seismic sources. In was the role of the SSFD Facilitation Team to compute these parameters using the methods and data that the SSFD expert teams specified. The results of these calculations for each team are presented as part of the description of their models. In addition, we employ the expert teams' models to compute the implied rate for future seismicity within 100 km of Yucca Mountain. Figure 4-15 shows the region for which this calculation is made. We present calculated earthquake recurrence rates for local seismic sources, which generally lie within the shaded region at the center of Figure 4-15, the regional faults that lie within a 100-km radius of Yucca Mountain, adjusting for the portions of these faults that may lie outside of this circle, and for those parts of the areal source zones that lie within 100 km of Yucca Mountain. The recurrence rates for the regional faults and the areal zones, as well as the combined recurrence rates for all three types of sources, are compared to the observed seismicity rate within the 100-km circle based on each SSFD team's selection of the appropriate earthquake catalog and catalog completeness periods. Shown on Figure 4-15 are the earthquakes of M_w 5 and larger that have been recorded within the 100-km circle. The choice of a 100 km radius encloses the region containing the seismic sources that will affect the seismic hazard at the Yucca Mountain site.

Arabasz, Anderson, Ramelli (AAR) Team. Tectonic models provide a fundamental framework for the AAR team's seismic source characterization for local sources. Many of their seismic source parameters are dependent on tectonic models, including the geometry of local faults and buried sources, rupture behavioral models for local faults, and the seismogenic potential of hypothesized buried sources. Figure 4-16a and 4-16b show the logic tree that defines the alternative interpretations of local faults developed by the AAR team. These models are based on the inference that the controlling tectonic model for the Crater Flat structural domain is simple shear. Figure 4-16a shows the logic structure for considering alternative models for local faults. The first assessment addresses whether or not a superposed NW-SE dextral shear is manifested as specific structures. If so, three alternative models for these structures are considered: (1) a regional throughgoing dextral shear zone subjacent to Yucca Mountain (Model A), (2) a right-stepping dextral shear zone that produces a pull-apart basin

without an underlying cross-basin fault (Model B), and (3) a right-stepping dextral shear zone that produces a pull-apart basin with an underlying cross-basin fault (Model C). The integral structures in all of these models are buried and/or hypothesized, with the possible exception of the Highway 95 (or Carrara) fault, which may form the southern boundary of the pull-apart basin in Models B and C. The locations of these sources are shown on Figure 4-17. The case with no specific dextral shear source is designated Model D. The Highway 95 fault and the north-bounding fault are assessed to have less than 1.0 probability of being seismogenic.

The possible existence of a local detachment zone was considered, with the likelihood that the detachment exists dependent on the existence of cross-basin shear structures (Figure 4-16a). Although not considered to be seismogenic, the detachment zone controls the down-dip extent of all local faults, except the Bare Mountain fault, and hypothesized buried dextral shear structures. Possible depths for detachments range from 3 km to the maximum thickness of the seismogenic crust. Under the assumption that a detaching layer does not exist, the down-dip extent of the local faults is controlled by the Bare Mountain fault and the thickness of the seismogenic crust.

The AAR team distinguished two parameters for the maximum depth of the seismogenic crust: (1) DMAX1 constrains down-dip extent of fault rupture for calculating rupture area to be used with empirical relations for estimating M_{max} and (2) DMAX2 is the maximum depth of seismogenic rupture during larger earthquakes, in which case rupture area is entered into an equation for seismic moment to estimate M_{max}. DMAX1 was assessed to range from 11 km to 17 km, based on the depth distribution of seismicity in the southern Great Basin, and represents the nominal definition of maximum depth defined in Wells and Coppersmith (1994). DMAX2, ranging from 14 km to 22 km, is based on the assessment that longer ruptures ($\geq$ 25 km) extend below the seismogenic crust into the brittle-ductile transition zone.

Two alternative modes of behavior were assessed for the local fault sources (Figure 4-16b). The first considered the local faults to act as independent sources. Figure 4-18 shows the locations of these faults. Some of these sources were considered to be potentially linked along strike into larger faults (the Paintbrush Canyon-Stagecoach Road system and the Southern, Central, Northern Windy Wash-Fatigue Wash system). The alternative considered that all of the observed normal faults in the Yucca Mountain area coalesce at depth into one to four master

faults (Figure 4-19). In general, coalesced behavior is favored over independent behavior, with the specific weight dependent upon the existence and depth of potential detachments. When the number of coalesced faults is less than four, then it is assumed that large earthquakes produce comparable amounts of slip on parallel fault traces during a single earthquake. Under the assumption of independent fault behavior, the minor faults such as the Ghost Dance, west Dune Wash, and Crater Flat) are assessed to have less than 1.0 probability of being seismogenic.

M_{max} for the local sources was based on empirical relationships between magnitude and rupture length, rupture length and slip rate, rupture area, and on estimation of seismic moment. The assessed distributions for M_{max} are shown on Figure 4-20. The AAR team chose to follow the convention developed by Youngs *et al.* (1987) in developing recurrence relationships for the faults. Following this approach, M_{max} assessed from the various empirical relationships is considered the central value of the characteristic magnitude interval, which is $M_{max} \pm ¼$ magnitude units. The upperbound magnitude of the recurrence relationship, m^U, is thus equal to $M_{max} + ¼$. The magnitudes plotted on Figure 4-20 are m^U.

Earthquake recurrence relationships for the local faults were based on assessments of slip rates and the recurrence intervals of large earthquakes (when data are available for a specific fault), with slip rate slightly favored. Slip rates of individual faults were summed across strike to assess rates for coalesced systems. A characteristic recurrence model was favored over a modified exponential model.

The AAR team identified 19 regional fault sources (Figure 4-21). The potential for two faults to be linked together into a single fault system was considered for the Death Valley and Furnace Creek faults, and for the Amargosa River and Pahrump faults. Preferred dips were generally 65° for normal faults and 90° for strike-slip faults. M_{max} for the regional sources were based on empirical relationships between magnitude and rupture length, rupture length and slip rate, and rupture area. The assessed distributions for M_{max} are shown on Figure 4-22. These values again are $M_{max} + ¼$. Earthquake recurrence relationships for the individual faults were assessed using the approaches outlined above for the local faults.

The AAR team defined regional source zones to account for the potential occurrence of earthquakes on faults not specifically identified as potential sources or unknown faults. Figure

4-23 shows the logic tree that defines the alternative interpretations of regional zones. Three alternatives were considered for defining these zones in which the spatial distribution of seismicity was assessed to be uniform (Figure 4-24). A fourth alternative was to use the kernel density estimation technique (discussed in Section 4.1.2) to define the spatial distribution of earthquakes within 100 km of Yucca Mountain without imposing source zone boundaries. The potential occurrence of volcanic-related earthquakes was addressed by the regional zones.
The M_{max} assessed for the regional zones ranged from M_w 6.6 to 7.3. Because of greater confidence in the identification and characterization of fault sources in the immediate Yucca Mountain vicinity, M_{max} was assessed to range from M_w 6.0 to 6.6 for the areal zone within 20 km of the Yucca Mountain site. The AAR team used the catalog of independent events produced by the declustering method of Veneziano and van Dyck (1985). The recurrence relationships for the individual source zones were estimated using the approach described in Section 4.1.4.1. All earthquakes occurring in the underground nuclear explosion (UNE) zone post-1950 were removed from the recurrence calculation. Figure 4-25 shows the recurrence relationships for each of the regional zones. These relationships were obtained using the maximum likelihood techniques discussed in Section 4.1.4.

The seismic source models developed by the AAR team can be used to calculate earthquake recurrence relationships (Figure 4-26) for the area shown on Figure 4-15. Plot (a) shows the distribution of earthquake frequencies computed using the AAR model for local faults (Figures 4-17 through 4-19). This distribution of earthquake occurrence rates applies to the area approximated by the shaded region around Yucca Mountain shown on Figure 4-15. The AAR local fault model contains about one and one-half orders of magnitude uncertainty in the combined recurrence rate for the local sources.

Plot (b) shows the distribution of earthquake frequencies computed using the AAR model for regional faults (Figure 4-21). Occurrence rates were computed for those portions of the regional faults that lie within 100 km of the Yucca Mountain site. The uncertainty in the recurrence rate for the regional faults is significantly smaller than that for the local faults. It should be noted that for all of the expert team characterizations, the predicted recurrence rates for regional faults are dominated by those estimated for the Death Valley and Furnace Creek faults. Also shown on Plot (b) are the observed frequencies of earthquakes occurring within

100 km of the Yucca Mountain site. Most of the smaller earthquakes are not close to the regional faults.

Plot (c) shows the distribution of earthquake frequencies computed using the AAR model for regional source zones (Figure 4-24). Again, the occurrence rates were computed for those portions of the regional source zones that lie within 100 km of the Yucca Mountain site. The uncertainty in the recurrence rate for the regional sources zones is also significantly smaller than that for the local fault sources. Also shown on Figure 4-26 are the observed frequencies of earthquakes occurring within the same region. (These are the same frequencies as those shown on Plot [b].) The predicted earthquake frequencies for the regional zones are somewhat greater than the observed frequencies because they are based on larger source areas that include regions of higher seismicity rates that lie beyond the 100-km circle.

Plot (d) shows the distribution of earthquake frequencies computed for all the sources in the AAR seismic source model for the region that lies within 100 km of the Yucca Mountain site compared to the observed earthquake frequencies. There is reasonable agreement between the observed and predicted rates for magnitudes of interest to the ground motion hazard assessment.

Ake, Slemmons, McCalpin (ASM) Team. The ASM team incorporates various aspects of planar fault block, detachment, lateral shear, and volcanic-tectonic models into their characterization of the local seismic sources. Figures 4-27a and 4-27b show their logic tree defining the uncertainties in characterizing the local faults. The locations of these faults are shown on Figures 4-28 and 4-29. The ASM team considers the possibility of the existence of a regional detachment underlying Yucca Mountain, although their preferred tectonic model is that the faults are planar to a depth controlled by the brittle-ductile transition and the Bare Mountain fault. The regional detachment has a very low probability (0.01) of being seismogenic and may lie at three alternative depths: 6 km, halfway between 6 km and the brittle-ductile transition (preferred), and at the brittle-ductile transition. The brittle-ductile transition is assessed to lie in the depth range of 12 to 17 km. They also consider the potential for the existence of a buried strike-slip fault, with the probability that it exists dependent on the existence of a regional detachment. The probability that a buried strike-slip fault is seismogenic depends on its minimum depth, which is controlled by the depth of the detachment (Figure 4-27).

The ASM team identified 10 local faults as seismic sources near Yucca Mountain (Figure 4-28). Five of these faults (Bare Mountain, Windy Wash, Solitario Canyon, and Paintbrush Canyon/Stagecoach Road) are termed major, block-bounding faults, and are assessed to be seismogenic. The remaining faults (Northern and Southern Crater Flat, Fatigue Wash, Iron Ridge, and Bow Ridge) are interpreted to be minor or secondary faults and have a probability of being seismogenic less than 1.0.

Two alternative geometries are considered for the local faults: planar and merging down dip. Under the planar assumption, the major faults penetrate to the base of the seismogenic crust and the down-dip extent of the minor faults is controlled by an aspect ratio of 1.5. Under the merging down-dip assumption, the major faults are truncated by the Bare Mountain fault or the detachment (if it exists) and the minor faults merge with the major faults. Three alternative geometries are assessed for this merging system: shallow, intermediate, and deep merging depths.

Two alternative behaviors were considered for the case of merging faults: the principal faults always rupture independently (the preferred model) and sometimes the principal faults rupture simultaneously (Figure 4-27b). Specific fault rupture combinations and the fraction of fault ruptures that are simultaneous ruptures were assessed by the ASM team.

The M_{max} for the local fault sources was assessed using empirical relationships between magnitude and surface rupture length, maximum displacement, rupture length times maximum displacement, average displacement, and rupture area (depending upon the available data). Only combined rupture area was used to assess the magnitude of multiple fault ruptures. The resulting M_{max} probability distributions are shown on Figure 4-30.

The ASM team used the convention of Youngs *et al.* (1987) in developing recurrence relationships for the faults, with the upperbound magnitude of the recurrence relationship, m^u, equal to M_{max} obtained from the empirical relationships plus ¼ magnitude units. The magnitudes plotted on Figure 4-30 are m^U. The rates of seismic activity on the local sources were assessed using fault slip rate and large magnitude earthquake recurrence interval approaches (depending on available data). For the mapped normal faults, the characteristic recurrence model was favored (0.7) with lesser weight given to the truncated exponential (0.2)

and maximum moment (0.1) recurrence models. Only the characteristic recurrence model was used for the detachment and buried strike-slip sources and the simultaneous rupture of multiple faults was assessed to conform to the maximum moment recurrence model.

Figure 4-31 shows the 26 regional fault sources characterized in the ASM seismic source models. With the exception of the Carrara (Highway 95) fault, these faults are assigned a probability of 1.0 of being seismogenic based on paleoseismic evidence. The sources are modeled as planar faults that extend to the depth of the brittle-ductile transition. Generalized dips of 90° for strike-slip faults and 60° for normal faults were used. M_{max} was assessed based on an assessed distribution for maximum surface rupture length. The resulting M_{max} probability distributions are shown on Figure 4-32. Again, these magnitudes are M_{max} + ¼. Rates of seismicity were assessed based on fault slip rate and estimates of the recurrence intervals for surface-rupturing earthquakes. A maximum moment model was strongly favored (0.8) over a characteristic recurrence model (0.2).

The ASM team defined six regional source zones to account for the potential occurrence of earthquakes on faults not specifically identified as potential sources. Figure 4-33 shows the logic tree that defines the alternative interpretations of the regional source zones shown in Figure 4-34. Volcanic-related earthquakes were not modeled as a separate source, but rather were modeled as part of the earthquakes occurring in the areal source zones.

The M_{max} assessed for the regional zones ranged from M_w 6.5 to 7.2. Because of the greater detail of fault investigations and seismic source characterization in the immediate Yucca Mountain vicinity, M_{max} was assessed to range from M_w 6.0 to 6.6 within 50 km of the Yucca Mountain site. The ASM team used the catalogs of independent events produced by the declustering methods of Youngs *et al.* (1987) and Veneziano and van Dyck (1985). The recurrence relationships for the individual source zones were estimated using the approach described in Section 4.1.4.1. All earthquakes occurring in the UNE zone post-1950 were removed from the recurrence calculation. Figure 4-35 shows the recurrence relationships for each of the source zones.

Figure 4-36 shows the distribution for earthquake recurrence predicted by ASM seismic source characterization for local faults, regional faults, regional zones, and all sources

combined compared to the observed frequency of earthquakes occurring within 100 km of the Yucca Mountain site. The ASM local fault model contains about one and one-half orders of magnitude uncertainty in the combined recurrence rates. A significant part of this uncertainty is due to differences between the recurrence rates assessed using fault slip rate and those assessed using paleoseismic recurrence intervals. The uncertainty in the recurrence rate for large earthquakes occurring on the regional faults is much smaller than that for smaller earthquakes because of the range in earthquake recurrence models used by the ASM team. It should be noted that the use of the maximum moment model for regional fault recurrence does not imply a complete absence of smaller-magnitude earthquakes on or in the immediate vicinity of these faults. The fault sources are superimposed on regional source zones. Thus, the use of a maximum moment recurrence model for the regional faults implies that the occurrence rate for smaller earthquakes is no larger on the fault than at other locations within the regional zone. Within 100 km of Yucca Mountain, the predicted earthquake frequencies for the regional zones are somewhat greater than the observed frequencies, because they are based on larger source areas that include regions of higher seismicity that lie beyond the 100-km circle. The predicted occurrence rates from all sources for earthquakes of interest to the hazard assessment generally fall within the uncertainties in the observed rates.

Doser, Fridrich, Swan (DFS) Team. The DFS team does not specifically address tectonic models in developing an overview model for seismic source characterization, but rather uses aspects of various structural models to estimate the location, style of faulting, and down-dip geometry of local fault sources and hypothetical faults near the site. Figure 4-37 shows the logic tree developed by the DFS team to address uncertainties in defining and characterizing the local faults. Two alternative modes of behavior are considered for the local fault sources: (1) independent fault behavior, which is strongly preferred (weight 0.95), and (2) distributed fault behavior (0.05) (Figure 4-37a). The locations of the independent fault sources are shown on Figure 4-38. The Ghost Dance fault is included as a possible independent fault with a low probability of activity (0.05). The distributed fault behavior model allows for simultaneous rupture on subparallel faults, including faults on either side of Yucca Mountain. The pattern of fault rupture given the distributed fault behavior model varies from single to quadruple parallel ruptures depending on the inferred length of fault rupture. Alternative assessments are defined for the total length of distributed faulting (Figure 4-37b) and for the total length of individual

faults (Figure 4-37c). The assessed distributions of maximum rupture length for individual faults depend on the total fault length (Figure 4-37c).

The next assessment in the logic tree addresses the existence of a detachment. The preferred model (weight 0.8) is that the faults are planar to the base of the seismogenic crust (inferred to be at a depth in the range of 12 to 16 km) The alternative model (weight 0.2) is that the Paintbrush Canyon fault becomes listric at depth, forming a detachment. All of the west-dipping faults at Yucca Mountain are assumed to truncate against the east-dipping Bare Mountain fault. Two alternative structural models are used to define the down-dip geometry of the planar faults and a single model is used to define the down-dip geometries for the detachment model. These geometries are shown in the DFS elicitation summary (Appendix E). The detachment model allows for the possibility of a seismogenic detachment, whereby the Paintbrush Canyon/Stagecoach Road fault is modeled as a shallow-dipping seismogenic source that extends beneath the Crater Flat Basin. The detachment model also allows for the possibility of the existence of a buried strike-slip fault of local (weight 0.5) or regional (weight 0.5) extent. Figure 4-39 shows the location of the hypothesized buried strike-slip fault. The three traces indicate alternative locations for the source. Also shown on Figure 4-39 is the location of the hypothesized Highway 95 fault.

The methods used to calculate M_{max} for the local faults were empirical relations between magnitude and rupture length and area. Figure 4-40 shows the resulting M_{max} probability distributions. The DFS team considered the magnitude estimated from the empirical relationships to be the upperbound magnitude of the recurrence relationships, but included an uncertainty of ±¼ magnitude units about these estimates in forming their M_{max} distributions. The recurrence relationships for the local faults were based on estimates of slip rates. Three recurrence models were used for the local faults: exponential, characteristic, and maximum moment, with the characteristic earthquake model preferred (weight 0.6). The weights assigned to the two other models are conditional on the fault behavior model for the local faults. The maximum moment model is given greater weight in the independent rupture model (Figure 4-37c) and a weight equal to the exponential model in the distributed model (Figure 4-37b).

The DFS team included 18 regional faults that are judged to be capable of generating M_w 5 or larger earthquakes and inferred to have had multiple late Quaternary displacements. These sources are shown on Figure 4-41. All these faults are considered active with a probability of 1.0 and are characterized as planar faults extending to the maximum seismogenic depth with dips dependent on the style of faulting (90° for strike-slip faults, 60° for dip-slip faults). M_{max} were calculated using empirical relationships between magnitude and fault rupture lengths and rupture areas. Figure 4-42 shows the resulting M_{max} probability distributions. Earthquake recurrence relationships for the regional sources were based on estimates of fault slip rates. The same three earthquake recurrence models used for the local faults were used for the regional sources.

Figure 4-43 shows the logic tree used to define the uncertainty in characterizing the regional source zones. The DFS team considered two alternative source zone models: Model A (weight 0.2), which consists of one regional zone, and Model B (weight 0.8), which has three regional zones. Figure 4-44 shows the configurations of these regional zones. The spatial distribution of earthquakes within these regional zones is interpreted to either conform to the existing pattern of seismicity, estimated using kernel spatial density estimation, or to be uniform, with the nonuniform pattern preferred.

The M_{max} assessed for the regional source zones ranged from M_w 7.0 to 7.7. Because of the greater detail of fault investigations and seismic source characterization in the immediate Yucca Mountain vicinity, M_{max} was assessed to range from M_w 5.6 to 6.0 within the local zone shown on Figure 4-44. The DFS team used the catalogs of independent events produced by the declustering methods of Youngs *et al.* (1987) and Veneziano and van Dyck (1985). The recurrence relationships for the individual source zones were estimated using the approach described above in Section 4.1.4.1. Earthquakes that occurred in close proximity to the regional faults were assumed to be associated with those sources and were not included in the data used to compute the seismicity rates for the regional zones. Figure 4-45 shows the recurrence relationships for each zone.

Figure 4-46 shows the distribution for earthquake recurrence predicted by the DFS team's seismic source characterization for local faults, regional faults, regional source zones, and all sources combined compared to the observed frequency of earthquakes occurring within 100

km of the Yucca Mountain site. The DFS local fault model contains about one and one-half orders of magnitude uncertainty in the combined recurrence rates. A significant part of this uncertainty is due to differences in predicting the frequency of earthquakes smaller than the maximum based on alternative recurrence models. The uncertainty in the recurrence rate for the regional faults is similar to that for the local faults, and also has a significant component contributed by the alternative recurrence models considered to estimate the frequency of earthquakes smaller than the maximum. Within 100 km of Yucca Mountain, the predicted earthquake frequencies for the regional zones are somewhat higher than the observed frequencies, because they are based in part on larger source areas that include regions of higher seismicity rates that lie beyond the 100-km circle. The predicted occurrence rates from all sources for earthquakes of interest to the hazard assessment generally fall within the uncertainties in the observed rates.

Rogers, Yount, Anderson (RYA) Team. The RYA team states that none of the tectonic models that have been proposed provide a unified explanation of all the available seismic, geologic, and geophysical data for Yucca Mountain and the larger Walker Lane. Therefore, they do not specifically address tectonic models in developing an overview seismic source model. Rather, they use aspects of various structural models to estimate the location, style of faulting, and down-dip geometry of local fault sources and hypothetical faults near the site. Figure 4-47 shows the logic tree used by the RYA team to describe the uncertainty in characterizing the local faults. The basic model is a system of from one to three west-dipping, coalescing faults and the east-dipping Bare Mountain fault (Figure 4-48). The weight assigned to the existence of one, two, or three faults depends upon the thickness of the seismogenic crust, which is assessed to be in the range of 12 to 20 km.

M_{max} for the local faults was estimated using empirical relationships between magnitude and surface rupture length and rupture area. The RYA team considered the magnitude estimated from the empirical relationships to be the upperbound magnitude of the recurrence relationships, but included an uncertainty of ± ½ magnitude units about these estimates in forming their M_{max} distributions. The resulting M_{max} probability distributions are shown on Figure 4-49. Earthquake recurrence rates for the local faults were based on trench recurrence interval data and slip-rate data, with a preference for the slip-rate approach. Characteristic and truncated exponential recurrence models were used. The weight assigned to each model was

dependent on the number of coalescing faults, with increasing preference for the exponential model as the number of independent sources decreased.

The RYA team defined 11 regional faults (Figure 4-50). These faults all are considered active with a probability of 1.0. Regional faults are treated as steeply-dipping planar faults penetrating to the maximum thickness of the seismogenic crust, with dips depending on the style of faulting (90° for strike-slip faults, 60° for normal faults). M_{max} for the regional faults were estimated using empirical relationships between magnitude and surface rupture length, rupture area, and maximum displacement, depending upon the available data. The resulting M_{max} probability distributions are shown on Figure 4-51. Earthquake recurrence relationships for the regional faults were estimated using estimates of fault slip rate . The characteristic and the truncated exponential recurrence models were used, with the characteristic model strongly preferred. In addition, the earthquakes occurring on the regional faults were limited to M_w 6.3 and larger. The occurrence of earthquakes smaller than M_w 6.3 was accounted for by the areal source zones. This approach is based on the concept that earthquakes smaller that M_w 6.3 do not occur on the faults with any greater frequency than elsewhere in the regional source zones.

Figure 4-52 shows the logic tree developed by the RYA team to describe the uncertainty in characterizing regional source zones. The RYA team divided the region within a 100-km radius surrounding Yucca Mountain into three primary seismic source zones with two alternate zonations (Scenarios 1 and 2) used to model a local source (Figure 4-53). The spatial distribution of earthquakes was assessed to be either uniform or nonuniform, with the latter based on a kernel density estimation using historical seismicity.

The M_{max} assigned to each of the areal zones is M_w 6.3 ± 0.3. The recurrence rates for the source zones were estimated by fitting truncated exponential relationships to simulations of the declustered catalogs. The technique used and results are described in the RYA team elicitation summary (Appendix E).

The RYA team also included in their seismic source model a volcanic source that encompasses the area of younger volcanism in the Yucca Mountain region and extends north to include Thirsty Mesa and Buckboard Mesa. They assess the probability that a separate volcanic source

exists to be 0.7. The recurrence rate is based on the estimated return period for volcanic events (assessed to be 2×10^5 years to 2×10^6 years) and M_{max} was assessed to be M_w 5.5.

Figure 4-54 shows the distribution for earthquake recurrence predicted by the RYA team's seismic source characterization for local faults, regional faults, regional source zones, and all sources combined compared to the observed frequency of earthquakes occurring within 100 km of the Yucca Mountain site. The RYA local fault source model contains about one order of magnitude uncertainty in the combined recurrence rates. The uncertainty in the recurrence rate for the regional faults is similar to that for local faults. As discussed above, the regional zones are used to model the occurrence of earthquakes smaller than M_w 6.3 on or near the regional faults. The RYA team used only the recorded earthquakes within 100 km of Yucca Mountain to evaluate the recurrence rate for the regional zones, thus there is good agreement between predicted and observed earthquake frequencies for the regional zones. The predicted occurrence rates for all sources for earthquakes of interest to the hazard assessment generally fall within the uncertainties in observed rates.

Smith, Bruhn, Knuepfer (SBK) Team. The SBK team considered a variety of tectonic models in the development of their seismic source model. Local seismic sources are characterized based on their strongly preferred oblique-rift/planar-fault model, with other tectonic models considered as constraints on source geometry and the potential for existence of hidden seismic sources. In this model, 3-D strain in the Yucca Mountain region is accommodated by normal-slip, strike-slip, and oblique-slip on planar faults. The Bare Mountain (master) and Yucca Mountain (antithetic) faults form a half-graben, whereas the Rock Valley and Highway 95 faults act as accommodation zones. Other potential sources, such as detachment faults, buried dextral shear zones, and volcanic sources related to dike-injection were considered either not to be seismogenic (e.g., detachments) or to be covered by background earthquakes in areal source zones (e.g., buried dextral shear zones and volcanic sources) and, thus, were not explicitly modeled as specific seismic sources.

Figure 4-55 shows the logic tree developed by the SBK team to represent the uncertainty in characterizing the local sources (shown on Figure 4-56). Four alternative behavioral modes were considered for local faults. Independent behavior of the mapped faults was the favored model (weight 0.5). The next most favored behavior mode (weight 0.4) is that the major block-

bounding faults are linked along strike to form independent faults along with the Bare Mountain fault. The two additional, less-likely, modes entail all of the Yucca Mountain faults soling into a detachment between 5 km and the base of the seismogenic zone (0.01), and all of the Yucca Mountain faults coalescing at depth into a master block-bounding fault (0.09). For all four modes of behavior, the possibility of simultaneous rupture events triggered by volcanic activity is considered. The likelihood of this simultaneous rupture event is considered greater for the detachment and coalescing fault behavior modes (0.5) than for the linked and independent modes (0.1). Three alternative geometries that defined the down-dip extent of the Yucca Mountain faults were considered for all four behavior modes.

M_{max} for the local faults was estimated using empirical relationships between magnitude and surface rupture length, rupture area, and maximum displacement, as well as estimates based on evaluation of seismic moment (rupture area times average displacement) and static stress drop. The resulting M_{max} probability distributions are shown on Figure 4-57. The SBK team also used the convention of Youngs *et al.* (1987) in developing recurrence relationships for the faults, with the upperbound magnitude of the recurrence relationship, m^U, equal to M_{max} obtained from the empirical relationships plus ¼ magnitude unit. The magnitudes plotted on Figure 4-57 are m^U. Earthquake recurrence relationships for the local faults were estimated from fault slip rates and recurrence intervals, depending upon the available data. For nonsimultaneous ruptures on coalescing fault and detachment models, slip rates were summed along across-strike transects. Recurrence of simultaneous ruptures was assessed based on recurrence of volcanic eruptions in Crater Flat. The characteristic and truncated exponential recurrence models were used for all but the simultaneous rupture scenarios, with the truncated exponential model generally favored. The maximum moment recurrence model was used for the simultaneous rupture scenarios.

Sixteen regional faults (Figure 4-58) were included with assessed likelihoods of seismogenic activity ranging from 0.01 to 1.0. Regional faults were modeled as independent, planar sources extending to the maximum seismogenic depth (12 to 17 km). Fault dips were based on fault type: 60° for normal, 70° for oblique, and 90° for strike-slip. The SBK team considered the possibility of linked-fault behavior for the Death Valley-Furnace Creek-Fish Lake Valley system of faults. The preferred model is that the four faults, Southern Death Valley, Death Valley, Furnace Creek, and Fish Lake Valley, are independent faults. Approximately 0.05 probability is given to a model with two linked faults, and 0.01 probability is given to a model with all four

faults linked. M_{max} for the regional faults was evaluated using empirical relationships between magnitude and surface rupture length, rupture area, and maximum displacement, as well as estimates based on evaluation of seismic moment. The resulting M_{max} probability distributions are shown on Figure 4-59. Again, these are M_{max} + ¼. Both the slip rate and recurrence interval approaches were used to assess rates of seismic activity with the former being favored, but fault-specific weights were assigned depending on available data. A characteristic recurrence model was favored for range-bounding faults and a truncated exponential model was favored for other fault zones exhibiting distributed faulting on multiple traces.

Figure 4-60 shows the logic tree developed by the SBK team to represent the uncertainty in characterizing the regional source zones. Two alternative zonation models were considered (Figure 4-61): one consisting of three zones and one in which an additional Rock Valley zone is defined. The spatial distribution of seismicity within the source zones was assessed to be uniform.

The M_{max} for regional source zones was assessed to range from M_w 6.2 to 6.6. Because of the greater detail of fault investigations and seismic source characterization in the immediate Yucca Mountain vicinity, M_{max} was assessed to range from M_w 5.6 to 6.2 within the local zone shown on Figure 4-61. The SBK team used the catalogs of independent events produced by the declustering methods of Youngs *et al.* (1987) and Veneziano and van Dyck (1985). The recurrence relationships for the individual source zones were estimated using the approach described above in Section 4.1.4.1. Adjustments for the effects of UNEs were incorporated as an alternative assessment of the recurrence rates. Figure 4-62 shows the recurrence relationships for each of the regional zones.

Figure 4-63 shows the distribution for earthquake recurrence predicted by the SBK team's seismic source characterization for local faults, regional faults, regional source zones, and all sources combined compared to the observed frequency of earthquakes occurring within 100 km of the Yucca Mountain site. The SBK local fault model contains about one order of magnitude uncertainty in the combined recurrence rates. The uncertainty in the recurrence rate for the regional faults is similar to that for the local faults. The SBK team used only the recorded earthquakes within 100 km of Yucca Mountain to evaluate the recurrence rate for the regional zones, thus there is good agreement between predicted and observed earthquake frequencies for

the regional zones. The predicted occurrence rates for all sources for earthquakes of interest to the hazard assessment generally fall within the uncertainties in observed rates.

Smith, de Polo, and O'Leary (SDO) Team. The preferred tectonic model for Yucca Mountain proposed by the SDO team is that of a half-graben partly filled by a collapsed volcanic carapace. They acknowledge that the site region also may be experiencing a component of northwest-directed dextral shear that is either confined to Crater Flat Basin (i.e., the basin itself is becoming distorted because of distributed, regional shear), or less likely, is being accommodated by an external, discrete strike-slip fault. To account for the latter, they assign a relatively high (0.4) probability to a strike-slip fault within or proximal to Crater Flat Basin along the hingeline-Pahrump-Stewart Valley fault zone alignment. They give zero weight to detachment models.

Figure 4-64 shows the logic tree developed by the SDO team to characterize the local faults. The SDO team identified six major faults (Paintbrush Canyon, Stagecoach Road, Solitario Canyon, Iron Ridge, Fatigue Wash, and Windy Wash faults) (Figure 4-65). All of these faults with the exception of the Iron Ridge and Fatigue Wash faults are considered to be "block-bounding" faults, structures that define major tilted panels of the carapace and that probably penetrate to significant seismogenic depth without intersection. Several other faults (Bow Ridge, Ghost Dance, Abandoned Wash, Northern Crater Flat, and Southern Crater Flat faults) might penetrate the carapace, but were deemed not capable of an earthquake larger than the maximum background earthquake (M_w 6.2). Three alternative geometries were defined to represent the interaction between the east-dipping Bare Mountain fault and the west-dipping Yucca Mountain faults. The major faults, as well as the faults that are thought to be confined to the carapace, were included in six individual (single, discrete planes), nine linked (individual planes linked along strike by complex structure) and eight distributed (planes linked across dip) fault rupture scenarios. As indicated on Figure 4-64, these rupture scenarios are not alternatives. All rupture scenarios are assumed to occur. The SDO team established the frequency of rupture on a particular fault, such as Paintbrush Canyon, from paleoseismic data on the occurrence of past ruptures. For each paleoseismic rupture, they evaluated the likelihood that the event corresponded to various rupture scenarios (e.g., rupture of just the northern part of the Paintbrush Canyon fault, versus rupture of all of the Paintbrush Canyon fault, versus rupture of Paintbrush Canyon and Stagecoach Road faults). These assessments for each paleoevent

were used to estimate the relative frequency of the various rupture scenarios for each fault. The product of the relative frequencies for the rupture scenarios times the estimates for frequency of ruptures on the fault provide estimates for the frequency of occurrence of the individual rupture scenarios.

M_{max} for the local faults was evaluated based on empirical relationships between magnitude and surface rupture length, maximum displacement, rupture length times maximum displacement, and rupture area, as well as estimates of seismic moment. The resulting M_{max} probability distributions for local faults are shown on Figure 4-66. The SDO team also used the convention of Youngs *et al.* (1987) in developing recurrence relationships for the faults, with the upperbound magnitude of the recurrence relationship, m^U, equal to M_{max} obtained from the empirical relationships plus ¼ magnitude unit. The magnitudes plotted on Figure 4-66 are m^U. A characteristic recurrence model was favored (0.7) over a truncated exponential model (0.3) for predicting the frequency of smaller events. A minimum magnitude of M_w 6.2 was used in the recurrence assessment for the local sources.

As noted above, the SDO seismic source model includes a buried strike-slip fault source. The hingeline, which appears to represent the structural boundary to a zone of features suggestive of distributed dextral shear deformation, is chosen by the SDO team as the best candidate location for a buried strike-slip fault. This fault is shown as fault T6-SS on Figure 4-67. The preferred (27 km) and minimum (20 km) estimates for fault length are based on the postulated length of the hingeline in the Crater Flat area. They also allow for the possibility that the hingeline represents the northwestern extension of the Pahrump-Stewart Valley fault zone. In this case they infer a maximum length of 120 km. The buried strike-slip fault is treated in a similar fashion to the other regional faults discussed below.

Thirty-six regional faults were characterized as separate fault sources by the SDO team (Figure 4-67). Within 50 km of Yucca Mountain, all identified Quaternary and possible Quaternary faults capable of $M_{max} \geq 6.4 \pm 0.2$ were included. In the distance range of 50 to 100 km from Yucca Mountain, faults of lengths of 20 km or more were included. Two faults that generally lie beyond 100 km, the Panamint Valley fault zone and the Ash Hill fault zone, also were included for their potential long-period ground motion contribution. Of the 36 faults included, 24 are judged to be active with a probability of 1.0, and 12 were judged active with probabilities

ranging from 0.2 to 0.9. Regional faults are modeled as planar fault sources extending to the maximum seismogenic depth (assessed to be in the range of 14 to 19 km) with dips depending on the style of faulting (90° for strike-slip faults, 60° for normal faults).

M_{max} for the regional faults was assessed using empirical relationships between magnitude and surface rupture length, maximum displacement, rupture length times maximum displacement, and slip rate plus rupture length. Fault weights were assigned depending on available data. The resulting M_{max} probability distributions are shown on Figure 4-68. These are also M_{max} + ¼. A recurrence interval approach was used by the SDO team to assess recurrence for regional faults. Specifically, the method used involved estimating average surface displacement from the minimum, preferred, and maximum fault lengths using relationships from Wells and Coppersmith (1994), dividing average displacement per event by slip rate to get a slip accumulation time (average recurrence interval), and inverting this estimate to obtain an annual earthquake occurrence rate. The characteristic recurrence model was favored over the truncated exponential model. A minimum magnitude of M_w 6.2 was used in the recurrence assessment. The occurrence of earthquakes smaller than M_w 6.2 was accounted for by the areal source zones. This approach is based on the concept that earthquakes smaller that M_w 6.2 do not occur on the faults with any greater frequency than elsewhere in the regional source zones.

Figure 4-69 shows the logic tree developed by the SDO team to represent the uncertainty in characterizing the regional source zones. Eight independent source zones were defined. Three of these zones lie within 100 km of the site (Figure 4-70). The spatial distribution of seismicity within the source zones was assessed to be either uniform or spatially varying, based on the observed pattern of recorded seismicity.

The M_{max} for the regional source zones was assessed to be M_w 6.4 ± 0.2. The SDO team used the catalogs of independent events produced by the declustering methods of Youngs *et al.* (1987) and Veneziano and van Dyck (1985), as well as a specific set of aftershock criteria defined by the team. The recurrence relationships for the individual source zones were estimated using the approach described above in Section 4.1.4.1. Figure 4-71 shows the recurrence relationships for each of the source zones.

The SDO team included two volcanic earthquake sources related to basaltic volcanoes and dike-injection (Figure 4-72): one based on the NE alignment of approximately 1-million-year-old volcanic vents across Crater Flat, and a second based on the vent alignment that encompasses the approximately 70-ka-years-old Lathrop Wells volcanic vent. The M_{max} for a volcanic-related earthquake in these zones was assessed to lie in the range of M_w 5.5 to 6.0. A recurrence of two to three volcanic events per million years was used to estimate an activity rate for these zones.

Figure 4-73 shows the distribution for earthquake recurrence predicted by the SDO team's seismic source characterization for local faults, regional faults, regional source zones, and all sources combined compared to the observed frequency of earthquakes occurring within 100 km of the Yucca Mountain site. The SDO local fault source model contains about one order of magnitude uncertainty in the combined recurrence rates. The uncertainty in the recurrence rate for the regional faults is similar to that for the local faults. As discussed above, the regional zones are used to model the occurrence of earthquakes smaller than M_w 6.2 on or near the regional faults. The regional zones defined by the SDO team extended beyond the 100-km-radius circle about Yucca Mountain, but did not include the areas of higher seismicity to the northwest that were included by other teams in their Walker Lane regional source zones. Thus, the SDO team's predicted rate of seismicity for the regional source zones within 100 km of Yucca Mountain are in good agreement with the observed earthquake frequencies for the regional zones. The predicted occurrence rates from all sources for earthquakes of interest to the hazard assessment generally fall within the uncertainties in observed rates.

4.3.1.2 Summary of Expert Seismic Source Characterization Assessments. In this section we summarize the range of interpretations made by the expert teams regarding key components of their seismic source characterization models. This section is organized by the various types of sources included in the models: seismic source zones, regional faults, local faults, and other sources (including buried strike-slip fault sources, seismogenic detachment fault, and volcanic sources). A summary of the key components of each of the source models is provided in Table 4-1.

Areal Source Zones. Areal source zones were defined by all teams to account for background earthquakes that occur on potential buried faults or faults not explicitly included in their model.

Four teams (AAR, DFS, RYA, and SBK) included alternative models in their characterization of the areal zones within a 100-km radius of the Yucca Mountain site. The RYA team's model always includes three zones, but allows for different configurations of the zone that include the site. The other three teams (AAR, DFS, and SBK) considered models that include one to three areal zones. The ASM and SDO teams each presented a single model that included two and three zones, respectively. Four teams (AAR, ASM, DFS, and SDO) define areal zones that extend beyond 100 km of the Yucca Mountain site. Four teams (AAR, ASM, DFS, and SBK) defined a site region or zone solely for assigning a lower M_{max} to the area where more detailed investigations have been conducted and the inventory of fault sources is more complete.

All teams used the truncated exponential model to estimate earthquake recurrence rates within the areal source zones. In regard to processing the catalog, the declustering method of Veneziano and van Dyck (1985) (catalog version 7) and the method of Youngs *et al.* (1987 catalog version 5) were both used by five of the teams, one team (AAR) used only catalog version 7 and one team (SDO) also gave some weight to a third catalog (version 8) based on their own analysis of declustering and completeness. Three of the teams (AAR, ASM, and SBK) made adjustments for UNEs in relevant zones. Varying treatments of the background seismicity were included: (1) uniform smoothing of seismicity was used solely or given significant weight by most of the teams, and (2) nonuniform smoothing using Gaussian kernels having different smoothing distances was included by four teams.

The M_{max} distributions for the areal zones were based on the largest earthquake that could occur in the region either randomly and/or on a geologic structure that was not explicitly included in the seismic source model. As noted above, lower values were included in several models for the local area around the Yucca Mountain site.

Regional Fault Sources. Regional faults were treated in a similar fashion by all six teams. Regional faults were defined by most teams as faults within 100 km that were judged to be capable of generating earthquakes of M_w 5 or greater based primarily on fault length and Quaternary histories of multiple surface fault rupturing earthquakes. Paleoseismic data from Piety (1995) was used by all the teams to identify and characterize potential regional faults. Other sources, such as Anderson *et al.* (1995a, 1995b), H. L. McKague *et al.* (CNRWA, written communication, 1996), W. R. Keefer and S. K. Pezzopane (USGS, written communication,

1996), and Pezzopane (USGS, written communication, 1996) also were used to varying degrees by some of the teams. Many of the faults that H. L. McKague *et al.* (CNWRA, written communication, 1996) consider Type 1 faults were not judged relevant to the hazard analysis and were not included as fault sources by any of the teams because of their short length, distance from Yucca Mountain, and evidence that indicates that many of these faults either have no significant Quaternary displacement or are much shorter than previously thought.

The number of faults included in the seismic source models for the various teams ranged from 11 to as many as 36. This reflects the judgments of the teams regarding the activity of various faults. One team included only faults that were judged to be active with a probability of 1.0, whereas the other five teams also included faults that were judged to be active with probabilities of less than 1.0. All teams modeled the regional faults as simple, planar faults to maximum seismogenic depths with generalized dips depending on the style of faulting (90° for strike-slip faults, 60° or 65° for normal-slip faults). Alternative fault lengths were included for most of the faults by all teams.

A variety of empirical relations were used by the teams to estimate M_{max} for the regional faults. Two teams (ASM and DFS) used only surface rupture length relations, whereas the other four teams incorporated one or more other regression relations based on rupture area, maximum displacement, average displacement, rupture area times maximum displacement, and surface rupture length plus slip rate, depending on available data.

Two general approaches were used to estimate recurrence rates for the regional faults: slip rates and recurrence intervals. Two teams (DFS and RYA) relied strictly on the slip-rate approach, whereas three teams (AAR, ASM, and SBK) used both. The SDO team used only a recurrence interval approach based on dividing the fault slip rate by the displacement for the maximum event. Four different recurrence models were used by the various teams: the characteristic recurrence model was used by all teams with weights ranging from 0.2 to 0.9, four teams used the truncated exponential with weights ranging from 0.1 to 0.3, two teams used a maximum moment model, and one team used a modified exponential.

Local Fault Sources. Varying fault behavioral and structural models were employed by the teams to capture the full range of complex rupture patterns and fault interactions in the

characterization of local faults. A planar fault block model is preferred by most teams, with linkages along strike or coalescence down dip considered by all teams. Simultaneous rupture of multiple faults was included in all models and was variously referred to as simultaneous rupture models (ASM and SBK), synchronous behavior (AAR), distributed behavior (DFS and SDO), and coalescing models (AAR, SBK, and RYA). In general, preferred models for multiple fault rupture included two to four coalescing fault systems. Four teams (ASM, AAR, DFS, and SBK) used detachment models to constrain the extent and geometry of the local faults. Two teams (ASM and DFS) include detachment models in their source model with weights of 0.15 and 0.2, respectively, and use these models to both characterize local faults as well as seismogenic detachment fault sources. In the AAR model, the likelihood of existence of hypothesized, local detachments is dependent on the type of dextral shear structures assumed to be present. The SBK team gave very low weight (0.01) to a model in which the local faults sole into a detachment. The RYA and SDO teams excluded detachments in their source models.

A variety of empirical relations were used by the teams to estimate M_{max} on the local faults. At a minimum, the teams considered rupture length and rupture area relationships. Four teams also considered relationships based on maximum displacement, average displacement, rupture area times maximum displacement, surface rupture length plus slip rate , and seismic moment, depending on available data.

As was done for the regional faults, two general approaches were used to estimate recurrence rates for the local faults: slip rate s and recurrence intervals. Four teams (ASM, AAR, RYA, and SBK) used both approaches with equal weight, or favored the slip-rate approach. The DFS team relied strictly on the slip-rate approach, and the SDO team used only recurrence intervals. Four different recurrence models were used by the various teams: the characteristic recurrence model was used by all teams with weights ranging from 0.2 to 0.9, five teams used the truncated exponential with weights ranging from 0.1 to 0.8, two teams gave weight (0.1 to 0.8) to a maximum moment , and one team used a modified exponential model (weight 0.3).

Buried Strike-Slip Faults. The possibility that dextral shear is being accommodated in the Yucca Mountain region by a buried strike-slip fault was considered by all teams. Four teams included a regional buried strike-slip fault source with low probability. Two teams (AAR and DFS) included throughgoing regional dextral shear zones with fault lengths ranging from 50 to

100 km and 30 to 200 km, respectively. The AAR team included the regional strike-slip fault as part of their throughgoing dextral shear model (0.05). Both the DFS and ASM teams considered the possibility of a buried strike-slip fault source to be conditional upon the existence of a detachment. The ASM team also considered the probability that a buried strike-slip fault was seismogenic conditional upon the depth of the inferred detachment. They used lengths of 25 km (preferred) and 60 km to model their buried fault source. The SDO team included a discrete buried strike-slip fault, but argued that the hypothesized fault would not extend north of the Crater Flat Basin, they also preferred a relatively short length (27 km), but allowed for a longer rupture (120 km) along the Pahrump/Stewart Valley fault zone to the south. Two teams (RYA and SBK) did not explicitly include buried strike-slip fault sources. Although they do not preclude the possibility of a buried fault, they conclude that this source would be incapable of generating an earthquake larger than those associated with their regional source zones.

Seismogenic Detachment Fault Source. As noted previously five teams incorporated detachment models in their treatment of local fault sources. Only two teams (ASM and DFS) explicitly allow for the existence of a seismogenic detachment fault source in their detachment models, which are given low weights (0.15 and 0.2, respectively). In the DFS model, only a local detachment is considered, whereby the Paintbrush Canyon-Stagecoach Road fault system is modeled as a shallow-dipping seismogenic source. The ASM team allows for a larger detachment source (rupture area of 4000 $\forall$ 2000 km^2) in their model, but give very low weight to the possibility of a seismogenic detachment (0.1) given that a detachment exists (0.15).

Volcanic Sources. Seismicity related to volcanic processes, particularly seismicity related to basaltic volcanoes and dike-injection, was explicitly modeled in volcanic source zones by two teams (RYA and SDO). Volcanic-related earthquakes were not modeled as a separate source by the other four teams, but owing to the low magnitude and frequency of volcanic-related seismicity, were accounted for by the areal source zones.

The concept of a volcanic-tectonic earthquake whereby some surface-rupturing earthquakes in Crater Flat Basin are accompanied by dike-injection (i.e., the postulated 70 ka "ash event"), was explicitly modeled by only one team (SBK). All the other teams included the possibility of such an event indirectly as part of their simultaneous rupture models (variously referred to as

synchronous [AAR], distributive behavior [DFS], coalescing fault [RYA] rupture models) but did not necessarily tie it to volcanism.

Predicted Recurrence Relationships. Figures 4-74 through 4-77 compare the predicted mean recurrence rates developed by each team to the combined distribution in recurrence rates over all teams for local faults, regional faults, regional source zones, and all sources combined. The combined distributions were obtained by giving equal weights to the individual team distributions. As was the case for the results presented by each team, the recurrence rate for local sources is for the area approximated by the shaded region on Figure 4-15 and the recurrence rate for the regional faults, regional source zones, and all sources combined is for the region within 100 km of the Yucca Mountain site.

There is approximately an order of magnitude range in the overall uncertainty in recurrence rate for M_w 6 and larger earthquakes on the local faults (Figure 4-74). The range between the mean results for the six teams is about one-half the overall range. The uncertainty in the recurrence rate increases significantly for larger magnitudes, primarily due to differences between the expert teams' assessment of M_{max} for the local faults. Assessments that favor multiple-fault ruptures, the use of displacement-based estimates of M_{max}, and recurrence rates for maximum events based on paleoseismic recurrence intervals tend to produce larger M_{max} and higher overall recurrence rates for the local faults. Assessments that favor the use of M_{max} assessments based on rupture area and recurrence rates based on slip rate tend to produce smaller M_{max} and lower overall recurrence rates. The uncertainty in recurrence rate also increases somewhat for magnitudes less than M_w 6. This increase is due primarily to uncertainty in the form of the recurrence model (truncated exponential versus characteristic versus maximum M_w distributions).

The uncertainty in the recurrence rate for M_w 6 and larger earthquakes on the regional faults (Figure 4-75) is about the same as that for the local faults. However, the uncertainty does not increase for larger magnitudes, because these recurrence rates are controlled by the recurrence for the Death Valley-Furnace Creek system of faults, for which the six teams developed similar characterizations. The very large range in results for smaller magnitudes reflects how the teams characterized the recurrence model (magnitude distribution for the regional sources). The RYA and SDO teams made the assessment that moderate earthquakes would not occur on the

regional faults at a greater rate than predicted for the regional source zones and, thus, limited their recurrence models for the regional faults to earthquakes larger than M_w 6.3 and 6.2, respectively. The occurrence of smaller earthquakes on or near the regional faults was modeled by their regional source zones. The remaining four teams considered truncated exponential, characteristic, and M_w distributions, generally favoring the characteristic model. Thus the large range in recurrence rate for M_w 5 and smaller earthquakes shown on Figure 4-75 is somewhat artificial. The observed rate of earthquakes (Figure 4-75) was not used by any of the teams to characterize the regional faults.

The combined distribution and mean estimates for the individual SSFD teams for recurrence in the regional source zones within 100 km of the Yucca Mountain site is shown on Figure 4-76. The spread in recurrence rates in the M_w 4 to 5.5 range reflects the degree to which the teams based their characterizations on a uniform distribution of seismicity in regional zones that extend beyond the 100-km region. Seismicity zones that included the higher rate of seismicity occurring to the northwest tend to predict higher rates of seismicity than observed in the Yucca Mountain region. This is based on the assumption that larger regions are required to adequately characterize the seismicity rates. The large range in results for magnitudes greater than M_w 6 reflects the differences in how the teams assessed the M_{max} for the regional zones within 100 km of the site. Three teams allowed for the occurrence of earthquakes greater than M_w 7 on sources that were not characterized explicitly as regional or local faults, and three teams considered that the sources of these events were treated explicitly in their characterization of other sources. Thus, the differences between the individual team assessments shown on Figures 4-75 and 4-76 reflect, in part, how each team partitioned the seismic source characterization between regional faults and regional source zones.

Figure 4-77 compares the combined distribution for earthquake recurrence from all seismic sources and the mean results for the six expert team characterizations. There is generally less than an order of magnitude range in uncertainty in the estimation of regional seismicity rates. At smaller magnitudes, the range reflects the differences in how the teams characterize the regional source zones. The overprediction of the observed rate of M_w 4 to 5 earthquakes within 100 km of the site reflects the teams' general assessment that larger regions are needed to characterize the seismicity rates. At larger magnitudes, the assessments from the individual teams lie within the uncertainty in the occurrence rates of earthquakes based on the historical

record. As discussed above, the results shown on Figure 4-77 are for the entire region within 100 km of the Yucca Mountain site. It is expected that the ground motion hazard will be influenced largely (at least for high spectral frequency ground motions) by nearby seismic sources. Thus, the larger uncertainty in recurrence rates for the local sources (Figure 4-74) will have a significant effect on the uncertainty in the ground motion hazard.

4.3.2 Fault Displacement Hazard Characterization Models

The instructions given to the SSFD expert teams were to develop a fault displacement hazard characterization model that could be applied to any location within the Controlled Area at the Yucca Mountain site. To demonstrate the application of these models and to provide an estimate of the fault displacement hazard, nine demonstration points were selected (see Figure 4-9) for fault displacement hazard characterization. The points were selected to represent the expected range of fault displacement hazard conditions within the Controlled Area in terms of the types of features that may be encountered: block-bounding faults with greater than 50 m of cumulative offset that may be seismogenic, mapped intrablock faults with north-south and northwest-southeast strikes having a few to tens of meters of cumulative displacement, and features observed within the ESF that are likely to be encountered within the proposed repository block, ranging from small faults uncorrelated with surface feature to intact rock. The selected points are (Figure 4-9):

Point 1. A location on the Bow Ridge fault where it crosses the ESF. The Bow Ridge fault is a block-bounding fault that has been characterized by the SSFD expert teams as being a potentially seismogenic fault and/or to be part of a seismogenic fault system.

Point 2. A location on the block-bounding Solitario Canyon fault, which has been characterized by the expert teams as one of the longer seismogenic faults within the Yucca Mountain site vicinity.

Point 3. A location on the Drill Hole Wash fault where it crosses the ESF, which is one of the longer of the northwest-striking faults within the Yucca Mountain site vicinity.

Point 4. A location on the Ghost Dance fault, which is one of the longer north-south intrablock faults within the Controlled Area.

Point 5. A location on the Sundance fault within the proposed repository footprint west of the ESF. The Sundance fault is an intermediate size, northwest-trending intrablock fault.

Point 6. A location on a small fault mapped in bedrock on the west side of Dune Wash. This point represents a location on one of the many small north-south-striking intrablock faults that have been mapped at the surface of Yucca Mountain.

Point 7. A location approximately 100 m east of Solitario Canyon at the edge of the proposed repository footprint. Any one of four hypothetical conditions were assumed to exist at this location that are representative of features encountered within the ESF that are not directly correlated with specific features observed at the surface:

(a) A small fault having 2 m of cumulative displacement
(b) A shear having 10 cm of cumulative displacement
(c) A fracture having no measurable cumulative displacement
(d) Intact rock

Point 8. A location within the proposed repository footprint midway between the Solitario Canyon and Ghost Dance faults. The same four hypothetical conditions were assumed to exist here as at Point 7.

Point 9. A location in Midway Valley east of the Bow Ridge fault on an observed fracture having no measurable displacement in Quaternary alluvium.

4.3.2.1 Individual Expert Team Models. The fault displacement hazard assessment models developed by the six SSFD expert teams are described in this section along with how the models are to be applied to the nine demonstration points. Table 4-3 summarizes key points of the fault displacement hazard assessment models for each team. Note that many of the terms and parameters used in this section were previously defined in Section 4.2.

Arabasz, Anderson, Ramelli (AAR) Team. The AAR team's characterization of fault displacement hazard differentiates between those sites that are subject to potential principal faulting hazard and those sites that are subject to distributed faulting hazard.

Characterization for Sites of Potential Principal Faulting Hazard. Figure 4-78 presents the AAR team's logic tree for characterization of sites subject to principal faulting hazard. The AAR team considers both the earthquake and displacement approaches.

Earthquake Approach. In the earthquake approach, two contributions to hazard are included (indicated by the vertical line on the logic tree under sources of hazard): hazard from principal faulting due to the occurrence of earthquakes on the fault and distributed faulting hazard from earthquakes occurring on other seismic sources. The first assessment in the earthquake approach is an evaluation of whether or not the feature can experience principal faulting or distributed faulting, $P(C)$. Because the occurrence of principal faulting requires that the feature in question be seismogenic, $P(C)$ for principal faulting is equal to the probability that the fault is seismogenic, $P(S)$, which was assessed as part of the AAR team's seismic source characterization for the ground motion evaluation (see Section 4.3.1.1). The probability that the feature in question can experience distributed slip, $P(C)$, was assessed based on the orientation of the feature in the present stress regime and evidence for past movement.

The next assessment in the earthquake approach is an evaluation of the frequency of occurrence of earthquakes of various magnitudes on each of the seismic sources. The characterization of earthquake recurrence developed by the AAR team for the ground motion hazard assessment was used directly to define the distributions for earthquake occurrence frequency.

Given the occurrence frequency of earthquakes, the next assessment is the approach for evaluating the probability that slip will occur in a given event. For principal faulting, the AAR team assessed P_i(slip|event on i) using the focal depth randomization for each fault developed for the ground motion hazard assessment. Two alternative empirical models for the size of earthquake ruptures as a function of magnitude were used to develop the rupture depth distribution and the distribution for along-strike location of rupture: one that defines

rupture length as a function of earthquake magnitude and one that defines rupture area as a function of earthquake magnitude. An empirical distribution for aspect ratio was used to evaluate rupture width given rupture length or rupture area. For distributed faulting, the AAR team assessed P_i(slip|event on j) using the logistic regression model based on the mapped density of distributed ruptures. The data and resulting model are shown in Figure H-13c. When evaluating the potential distributed faulting events induced by earthquakes occurring within the regional source zones, it is assumed that the point of interest is equally likely to be located in the hanging wall or footwall of the rupture.

The conditional probability of exceeding a specified displacement, $P(D>d)$, was evaluated using the two-part method defined by Equation (4-19). For principal faulting the AAR team considered three alternative empirical relationships for estimating the maximum displacement *MD*: (1) a published empirical model based on earthquake magnitude, (2) a published empirical model based on rupture length, and (3) an empirical model based on fault rupture length developed by the AAR team from Yucca Mountain data. The location of the point of interest was assessed for each rupture to define the parameter x/L, and the distribution for D/MD was based on the analysis of historical ruptures shown on Figure 4-13. For distributed faulting, an empirical distribution for the ratio of maximum distributed displacement to maximum principal displacement was defined based on published data. This ratio, ranging from 0.2 to 0.7, was used to scale the estimated *MD* for the earthquake source to that for distributed rupture on the fault of interest. The distribution for D/MD shown on Figure H-6 was then used to compute the conditional probability of exceedance assuming $x/L = 0.5$ for the distributed rupture.

Displacement Approach. The displacement approach does not distinguish between principal and distributed ruptures. The first assessment in the logic tree (Figure 4-78) is an evaluation of the probability the feature can slip, $P(C)$. This assessment is the same as the assessment of $P(C)$ in the earthquake approach.

The AAR team uses estimates of fault slip rate and average displacement per event to obtain the frequency of displacement events [Equation (4-13)]. The slip-rate estimates are given by the seismic source characterization model developed by the AAR team. The assessment of the average displacement per event, $\bar{D}_E$, is based on the AAR team's evaluation of the

displacement data from trenching studies at Yucca Mountain. For each trenching site, they made an estimate of the expected maximum displacement in the maximum event, which they denote by MD^{max}. They then normalized the displacement data from the trench by this value and pooled the data from all trenches. The mean of the pooled data for D/MD^{max} is 0.83. The AAR team assesses the average displacement per event by estimating MD^{max} for the fault and then uses the expression $\bar{D}_E = 0.83\ MD^{max}$. In applying this approach, they consider three alternative approaches for estimating MD^{max}. The first is based on maximum rupture length and two alternative empirical relationships between rupture length and maximum slip: a published empirical model and an analysis of Yucca Mountain data performed by the AAR team. The second approach uses a scaling relationship between cumulative bedrock offset and average displacement per event developed by the AAR team. The third approach utilized the team's assessments of maximum displacements estimated from paleoseismic data as part of their seismic source characterization of the faults for the ground motion hazard assessment.

The final part of the displacement approach is the model for the conditional probability of exceedance. The AAR team found that the distribution of D/MD^{max} could be modeled by an exponential distribution (see Figure H-5), and utilized this distribution to assess $P(D>d)$.

Characterization for Sites of Only Potential Distributed Faulting Hazard. Figure 4-79 presents the AAR team's logic tree for characterization of sites subject to only distributed faulting hazard. The AAR team considers both the earthquake and displacement approaches and the hazard characterization model is similar to that for sites of principal faulting hazard (Figure 4-78). The differences between the approaches for hazard characterization at the two types of sites primarily reflect the types of data available.

Earthquake Approach. In the earthquake approach, the first assessment is an evaluation of whether or not the feature can experience distributed faulting, $P(C)$, which is assessed based on the orientation of the feature in the present stress regime. The next assessment in the earthquake approach is an evaluation of the frequency of occurrence of earthquakes of various magnitudes on each of the seismic sources. As was the case for sites subject to principal faulting hazard, the characterization of earthquake recurrence developed by the AAR team for the ground motion hazard assessment was used to define the distributions for